J|A|C|S ARTICLES

Published on Web 03/16/2010

Cationic Polymerization and Insertion Chemistry in the Reactions of Vinyl Ethers with (α-Diimine)PdMe$^+$ Species

Changle Chen, Shuji Luo, and Richard F. Jordan*

Department of Chemistry, The University of Chicago, 5735 South Ellis Avenue, Chicago, Illinois 60637

Received January 19, 2010; E-mail: rfjordan@uchicago.edu

Abstract: The reactions of (α-diimine)PdMe$^+$ species (**1**, α-diimine = (2,6-^{i}Pr$_2$−C$_6$H$_3$)N═CMeCMe═N(2,6-^{i}Pr$_2$−C$_6$H$_3$)) with vinyl ethers CH$_2$═CHOR (**2a**−**g**: R = ^{t}Bu (**a**), Et (**b**), SiMe$_3$ (**c**), SiMe$_2$Ph (**d**), SiMePh$_2$ (**e**), SiPh$_3$ (**f**), Ph (**g**); **2a**−**g**: R = ^{t}Bu (**a**), Et (**b**), SiMe$_3$ (**c**), SiMe$_2$Ph (**d**), SiMePh$_2$ (**e**), SiPh$_3$ (**f**), Ph (**g**)) were investigated. Two pathways were observed. First, **1** initiates the cationic polymerization of **2a**−**c** with concomitant decomposition of **1** to Pd^0. This reaction proceeds by formation of (α-diimine)PdR′(CH$_2$═CHOR)$^+$ π complexes (R′ = Me or CH$_2$CHMeOR from insertion), in which the vinyl ether C═C bond is polarized with carbocation character at the substituted carbon (C$_{int}$). Electrophilic attack of C$_{int}$ on monomer initiates polymerization. Second, **1** reacts with stoichiometric quantities of **2a**−**g** by formation of (α-diimine)PdMe(CH$_2$═CHOR)$^+$ (**3a**−**g**), insertion to form (α-diimine)Pd(CH$_2$CHMeOR)$^+$ (**4a**−**g**), reversible isomerization to (α-diimine)Pd(CMe$_2$OR)$^+$ (**5a**−**g**), β-OR elimination of **4a**−**g** to generate (α-diimine)Pd(OR)(CH$_2$═CHMe)$^+$ (not observed), and allylic C−H activation to yield (α-diimine)Pd(η^3-C$_3$H$_5$)$^+$ (**6**) and ROH. Binding strengths vary in the order **2a** > **2b** ∼ **2c** > **2d** ∼ **2g** > **2e** > **2f**. Strongly electron-donating OR groups increase the binding strength, while steric crowding has the opposite effect. The insertion rates vary in the order **3a** < **3b** < **3c** < **3d** < **3e** < **3f** < **3g**; this trend is determined primarily by the relative ground-state energies of **3a**−**g**. The β-OR elimination rates vary in the order O^{t}Bu < OSiR$_3$ < OPh. For **2d**−**g**, the insertion chemistry out-competes cationic polymerization even at high vinyl ether concentrations. β-OR elimination of **4**/**5** mixtures is faster for SbF$_6^-$ salts than B(C$_6$F$_5$)$_4^-$ salts. The implications of these results for olefin/vinyl ether copolymerization are discussed.

Introduction

The development of catalysts that are capable of polymerizing or copolymerizing functionalized vinyl monomers (CH$_2$═CHX) by insertion mechanisms would enable the synthesis of new polyolefins with enhanced properties.[1] The discovery by Brookhart and co-workers that (α-diimine)PdR$^+$ catalysts copolymerize ethylene and acrylate monomers to highly branched copolymers was a seminal development in this field.[2] More recently, several groups have shown that (*ortho*-phosphino-arenesulfonate)PdR catalysts copolymerize ethylene with acrylates, vinyl ethers, vinyl fluoride, acrylonitrile, vinyl acetate, and other comonomers to linear copolymers.[3] However, in other cases, it has been found that CH$_2$═CHX monomers deactivate olefin polymerization catalysts. Several common deactivation processes have been identified, including (i) coordination of the CH$_2$═CHX monomer to the L$_n$MR$^+$ active species through the X group rather than the C═C bond to form unreactive L$_n$MR(κ-X−XCH═CH$_2$)$^+$ adducts;[4] (ii) formation of L$_n$MCH(X)CH$_2$R species that are resistant to subsequent insertion reactions due to X chelation, which blocks the site required for monomer coordination,[5] and the electronic influence of the X substituent;[6] and (iii) β-X elimination of L$_n$MCH$_2$CHXR or L$_n$MCHRCH$_2$X species to form unreactive L$_n$MX species.[7] Moreover, metal catalysts can

(1) (a) Boffa, L. S.; Novak, B. M. *Chem. Rev.* **2000**, *100*, 1479. (b) Dong, J. Y.; Hu, Y. L. *Coord. Chem. Rev.* **2006**, *250*, 47. (c) Drent, E.; Budzelaar, P. H. M. *Chem. Rev.* **1996**, *96*, 663. (d) Müller, C.; Rieger, B. *Prog. Polym. Sci.* **2002**, *27*, 815. (e) Chung, T. C. *Prog. Polym. Sci.* **2002**, *27*, 39. (f) Ittel, S. D.; Johnson, L. K.; Brookhart, M. *Chem. Rev.* **2000**, *100*, 1169. (g) Sen, A. *Pure Appl. Chem.* **2001**, *73*, 251. (h) Chen, E. Y. X. *Chem. Rev.* **2009**, *109*, 5157. (i) Nakamura, A.; Ito, S.; Nozaki, K. *Chem. Rev.* **2009**, *109*, 5215.

(2) (a) Leatherman, M. D.; Svejda, S. A.; Johnson, L. K.; Brookhart, M. *J. Am. Chem. Soc.* **2003**, *125*, 3068. (b) Shultz, L. H.; Tempel, D. J.; Brookhart, M. *J. Am. Chem. Soc.* **2001**, *123*, 11539. (c) Gottfried, A. C.; Brookhart, M. *Macromolecules* **2001**, *34*, 1140. (d) Tempel, D. J.; Johnson, L. K.; Huff, R. L.; White, P. S.; Brookhart, M. *J. Am. Chem. Soc.* **2000**, *122*, 6686. (e) Johnson, L. K.; Killian, C. M.; Brookhart, M. *J. Am. Chem. Soc.* **1995**, *117*, 6414.

(3) (a) Drent, E.; van Dijk, R.; van Ginkel, R.; van Oort, B.; Pugh, R. I. *Chem. Commun.* **2002**, 964. (b) Vela, J.; Lief, G. R.; Shen, Z.; Jordan, R. F. *Organometallics* **2007**, *26*, 6624. (c) Guironnet, D.; Roesle, P.; Runzi, T.; Gottker-Schnetmann, I.; Mecking, S. *J. Am. Chem. Soc.* **2009**, *131*, 422. (d) Kochi, T.; Noda, S.; Yoshimura, K.; Nozaki, K. *J. Am. Chem. Soc.* **2007**, *129*, 8948. (e) Luo, S.; Vela, J.; Lief, G. R.; Jordan, R. F. *J. Am. Chem. Soc.* **2007**, *129*, 8946. (f) Weng, W.; Shen, Z.; Jordan, R. F. *J. Am. Chem. Soc.* **2007**, *129*, 15450. (g) Ito, S.; Munakata, K.; Nakamura, A.; Nozaki, K. *J. Am. Chem. Soc.* **2009**, *131*, 14606. (h) Skupov, K. M.; Marella, P. R.; Simard, M.; Yap, G. P. A.; Allen, N.; Conner, D.; Goodall, B. L.; Claverie, J. P. *Macromol. Rapid Commun.* **2007**, *28*, 2033. (i) Skupov, K. M.; Piche, L.; Claverie, J. P. *Macromolecules.* **2008**, *41*, 2309. (j) Newsham, D. K.; Borkar, S.; Sen, A.; Conner, D. M.; Goodall, B. L. *Organometallics* **2007**, *26*, 3636.

(4) (a) Wu, F.; Foley, S. R.; Burns, C. T.; Jordan, R. F. *J. Am. Chem. Soc.* **2005**, *127*, 1841. (b) Wu, F.; Jordan, R. F. *Organometallics* **2006**, *25*, 5631. (c) Yang, S.-Y.; Szabo, M. J.; Michalak, A.; Weiss, T.; Piers, W. E.; Jordan, R. F.; Ziegler, T. *Organometallics* **2005**, *24*, 1242.

(5) Williams, B. S.; Leatherman, M. D.; White, P. S.; Brookhart, M. *J. Am. Chem. Soc.* **2005**, *127*, 5132.

initiate undesired radical or ionic homopolymerization of CH_2═CHX monomers.[8,9]

Vinyl ethers (CH_2═CHOR) are attractive candidates for insertion copolymerization with olefins because their steric and electronic properties can be tuned by varying the R group, possibly enabling the deactivation reactions noted above to be avoided. Several potential problems can be anticipated for vinyl ethers in insertion polymerization. First, vinyl ethers are highly susceptible to cationic polymerization,[10] and electrophilic olefin polymerization catalysts are good cationic initiators.[11,12] For example, [(P∼N)PdMe(CH_3CN)][BF_4] (P∼N = *o*-C_6H_4(PPh_2)-(N═CHAr), Ar = C_6H_5, 4-F−C_6H_5) species initiate cationic polymerization of ethyl vinyl ether to generate poly(ethyl vinyl ether) with a molecular weight of ca. 8000.[11b] Second, vinyl ethers can coordinate to metals not only through the C═C bond, as in [NEt_4][$PtCl_3$(CH_2═CHOEt)][13] and $PdCl_2$[NMe_2CH_2-CMe_2(CH═CHOMe)],[14,15] but also through the OR group, as in$(C_5H_4Me)_2Zr(O^tBu)(\eta^1$-*O*-EtOCH═$CH_2)^+andRuH(CO)(P^tBu_2Me)_2$-($\eta^1$-*O*-EtOCH═$CH_2)^+$.[15c,16] Third, the insertion barriers for L_nMR'(CH_2═CHOR) species are predicted to be high. For example, the insertion barrier of (HN═CHCH═NH)PdMe(CH_2═CHOMe)$^+$ was calculated by DFT to be ca. 6 kcal/mol higher than that for (HN═CHCH═NH)Pd-Me(CH_2═CH_2)$^+$.[17] Nevertheless, insertions of vinyl ethers into metal hydrides, such as RuH(CO)(P^tBu_2Me)$_2$(η^2-CH_2Cl_2)$^+$, ($^tBu_3SiO$)$_3TaH_2$, and $Os_3H_2(CO)_{10}$, have been reported.[16,18,19] Also, CH_2═CHOEt inserts into the Pd−acetyl bond of [(P∼N)Pd($COCH_3$)(CH_3CN)][BF_4] to generate [(P∼N)Pd-CH(OEt)CH_2COCH_3][BF_4].[11b] Finally, $L_nMCH_2CH(OR)R'$ species formed by 1,2 insertion of L_nMR'(CH_2═CHOR) species may undergo β-OR elimination, which would terminate chain growth. Wolczanski showed that ($^tBu_3SiO$)$_3TaH_2$ undergoes 1,2 insertion of CH_2═CHOR (R = alkyl, Ph) to generate ($^tBu_3SiO$)$_3$TaH(CH_2CH_2OR) species, which undergo β-OR elimination. However, the β-OR elimination rate decreases as the size of R increases, and ($^tBu_3SiO$)$_3$TaH($CH_2CH_2O^tBu$) is stable.[18]

Recently, we reported that (α-diimine)$PdMe^+$ species (α-diimine = (2,6-$^iPr_2$−C_6H_3)N═CMeCMe═N(2,6-$^iPr_2$−C_6H_3)) copolymerize 1-hexene and CH_2═CHO$SiPh_3$ to $OSiPh_3$-substituted polyhexene (Scheme 1).[20] Alkyl vinyl ethers such as CH_2═CHO^{t}Bu are not suitable comonomers in this system due to competing cationic polymerization and Pd^0 formation. Phenyl vinyl ether is also unsuitable because (α-diimine)Pd(CH_2CHMeOPh)$^+$ species generated by CH_2═CHOPh insertion undergo rapid β-OPh elimination, ultimately forming (α-diimine)Pd(η^3-C_3H_5)$^+$, which is catalytically inactive, and PhOH. Further studies showed that (α-diimine)$PdMe^+$ species undergo up to three sequential insertions of CH_2═CHO$SiPh_3$, ultimately forming Pd allyl products (Scheme 2).[21] The product distribution is dependent on the anion.

In this paper, we describe a comprehensive study of the reactions of (α-diimine)$PdMe^+$ species with a set of vinyl ethers with varying steric and electronic properties, CH_2═CHOR (**2a**−**g**: R = ^{t}Bu (**a**), Et (**b**), $SiMe_3$ (**c**), $SiMe_2Ph$ (**d**), $SiMePh_2$ (**e**), $SiPh_3$ (**f**), Ph (**g**)). We first describe studies of the reaction of (α-diimine)$PdMe^+$ with excess **2a**−**g** to probe the potential

Scheme 1

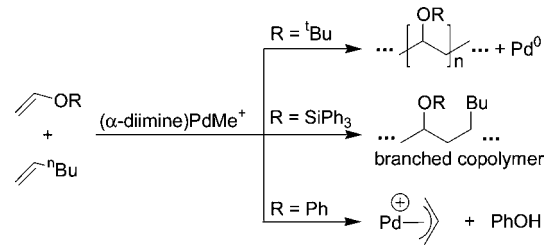

Scheme 2

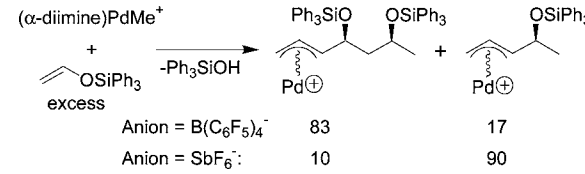

(6) (a) Foley, S. R.; Shen, H.; Qadeer, U. A.; Jordan, R. F. *Organometallics* **2004**, *23*, 600. (b) Philipp, D. M.; Muller, R. P.; Goddard, W. A.; Storer, J.; McAdon, M.; Mullins, M. *J. Am. Chem. Soc.* **2002**, *124*, 10198. (c) Szabo, M. J.; Jordan, R. F.; Michalak, A.; Piers, W. E.; Weiss, T.; Yang, S.; Ziegler, T. *Organometallics* **2004**, *23*, 5565. (d) Mitoraj, M.; Michalak, A. *J. Mol. Modeling* **2005**, *11*, 341.

(7) (a) Foley, S. R.; Stockland, R. A.; Shen, H.; Jordan, R. F. *J. Am. Chem. Soc.* **2003**, *125*, 4350. (b) Kang, M.; Sen, A.; Zakharov, L.; Rheingold, A. L. *J. Am. Chem. Soc.* **2002**, *124*, 12080.

(8) Stockland, R. A.; Foley, S. R.; Jordan, R. F. *J. Am. Chem. Soc.* **2003**, *125*, 796.

(9) (a) Schaper, F.; Foley, S. R.; Jordan, R. F. *J. Am. Chem. Soc.* **2004**, *126*, 2114. (b) Stojcevic, G.; Prokopchuk, E. M.; Baird, M. C. *J. Organomet. Chem.* **2005**, *690*, 4349.

(10) (a) Sawamoto, M. *Prog. Polym. Sci.* **1991**, *16*, 111. (b) Kennedy, J. P.; Iva'n, B. *Designed Polymers by Carbocationic Macromolecular Engineering: Theory and Practice*; Hanser: Munich, 1992. (c) Matyjaszewski, K. *Cationic Polymerizations*; Marcel Dekker: New York, 1996. (d) Katayama, H.; Kamigaito, M.; Sawamoto, M. *J. Polym. Sci., Part A: Polym. Chem.* **2001**, *39*, 1249. (e) Higashimura, T.; Sawamoto, M. In *Comprehensive Polymer Science Pergamon*; Allen, G., Bevington, J., Eds.; Oxford: U.K., 1989; Vol. 3, pp 673−696. Vinyl ethers are poor substrates for radical polymerization. See: (f) Matsumoto, A.; Nakane, T.; Oiwa, M. *Makromol. Chem., Rapid Commun.* **1983**, *4*, 277. (g) Kamachi, M.; Tanaka, K.; Kuwae, Y. *J. Polym. Sci., Part A: Polym. Chem.* **1986**, *24*, 925.

(11) (a) Baird, M. C. *Chem. Rev.* **2000**, *100*, 1471. (b) Chen, C. L.; Chen, Y. C.; Liu, Y. H.; Peng, S. M.; Liu, S. T. *Organometallics* **2002**, *21*, 5382. (c) Chen, Y. C.; Reddy, K. R.; Liu, S. T. *J. Organomet. Chem.* **2002**, *656*, 199. (d) Albietz, P. J., Jr.; Yang, K.; Lachicotte, R. J.; Eisenberg, R. *Organometallics* **2000**, *19*, 3543. (e) Albietz, P. J., Jr.; Yang, K.; Eisenberg, R. *Organometallics* **1999**, *18*, 2747. (f) Shaffer, T. D.; Ashbaugh, J. R. *J. Polym. Sci., Part A: Polym. Chem.* **1997**, *35*, 329. (g) Kawaguchi, T.; Sanda, F. O.; Masuda, T. *J. Polym. Sci., Part A: Polym. Chem.* **2002**, *40*, 3938.

(12) For vinyl ether polymerizations mediated by combinations of metal complexes and silanes, see: (a) Nagashima, H.; Itonaga, C.; Yasuhara, J.; Motoyama, Y.; Matsubara, K. *Organometallics* **2004**, *23*, 5779. (b) Crivello, J. V.; Fan, M. *J. Polym. Sci., Part A: Polym. Chem.* **1991**, *29*, 1853.

(13) Elder, R. C.; Pesa, F. *Acta Crystallogr.* **1978**, *B34*, 268.

(14) McCrindle, R.; Ferguson, G.; Khan, M. A.; McAalees, A. J.; Ruhl, B. L. *J. Chem. Soc., Dalton. Trans.* **1981**, *4*, 986.

(15) (a) Chang, T. C. T.; Foxman, B. M.; Rosenblum, M.; Stockman, C. *J. Am. Chem. Soc.* **1981**, *103*, 7361. (b) Watson, L. A.; Franzman, B.; Bollinger, J. C.; Caulton, K. G. *New J. Chem.* **2003**, *27*, 1769. (c) Stoebenau, E. J.; Jordan, R. F. *J. Am. Chem. Soc.* **2006**, *128*, 8162. (d) Song, J. S.; Szalda, D. J.; Bullock, R. M. *J. Am. Chem. Soc.* **1996**, *118*, 11134. (e) Cotton, F. A.; Francis, J. N.; Frenz, B. A.; Tsutsui, M. *J. Am. Chem. Soc.* **1973**, *95*, 2483. (f) Sartori, F.; Leoni, L. *Acta Crystallogr.* **1976**, *B32*, 145. (g) Pampaloni, G.; Peloso, R.; Graiff, C.; Tiripicchio, A. *Organometallics* **2005**, *24*, 4475.

(16) Huang, D.; Bollinger, J. C.; Streib, W. E.; Folting, K.; Young, V.; Eisenstein, O.; Caulton, K. G. *Organometallics* **2000**, *19*, 2281.

(17) Schenck, H.; Strömberg, S.; Zetterberg, K.; Ludwig, M.; Åkermark, B.; Svensson, M. *Organometallics* **2001**, *20*, 2813.

(18) Strazisar, S. A.; Wolczanski, P. T. *J. Am. Chem. Soc.* **2001**, *123*, 4728.

(19) Boyar, E.; Deeming, A. J.; Arce, A. J.; De Sanctis, Y. *J. Organomet. Chem.* **1984**, *276*, C45.

(20) Luo, S.; Jordan, R. F. *J. Am. Chem. Soc.* **2006**, *128*, 12072.

(21) Chen, C. L.; Luo, S.; Jordan, R. F. *J. Am. Chem. Soc.* **2008**, *130*, 12892.

cationic polymerization reactivity of these substrates. We then discuss the reactions of (α-diimine)PdMe$^+$ with 1 equiv of **2a**−**g**, under conditions where the concentration of vinyl ether is too low to support cationic polymerization, in order to probe the coordination, insertion, chain-walking, and *β*-OR elimination reactivity. These studies provide new insights to how to circumvent potential chemical obstacles to the insertion copolymerization of vinyl ethers and olefins.

Results

Generation of (α-Diimine)PdMe$^+$ (1). The cationic species (α-diimine)PdMe$^+$ (**1**) was generated by the methods shown in eq 1 and eq 2. The reaction of (α-diimine)PdMeCl and Ag[SbF_6] in Et_2O generates [(α-diimine)PdMe(OEt_2)][SbF_6] (**1**[SbF_6]), which was isolated as a yellow solid. **1**[SbF_6] is stable in CD_2Cl_2 at −60 °C for at least 12 h but decomposes slowly at 20 °C.[2d,22] The Et_2O ligand is readily displaced by vinyl ethers to generate [(α-diimine)PdMe(CH_2═CHOR)][SbF_6] (**3**[SbF_6]) vinyl ether adducts.

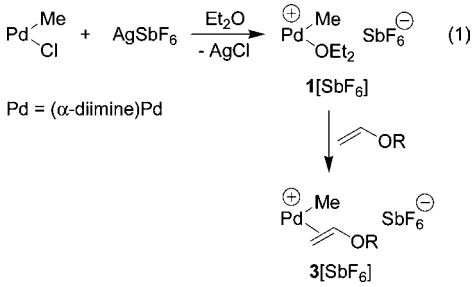

Alternatively, (α-diimine)PdMe$^+$ was generated in situ by the reaction of (α-diimine)PdMeCl and [Li(Et_2O)$_{2.8}$][$B(C_6F_5)_4$] in CD_2Cl_2 at 20 °C (eq 2). In the absence of Lewis bases, this reaction produces the dinuclear species [{(α-diimine)PdMe}$_2$(*μ*-Cl)][$B(C_6F_5)_4$], which is stable at 20 °C at least for 24 h, along with an equimolar amount of unreacted [Li(Et_2O)$_{2.8}$][$B(C_6F_5)_4$].[4a] In the presence of Lewis bases (L) that are sufficiently strong to displace (α-diimine)PdMeCl from [{(α-diimine)PdMe}$_2$(*μ*-Cl)]$^+$, (α-diimine)PdMe(L)$^+$ species are formed. This in situ generated cationic system will be referred to as **1**[$B(C_6F_5)_4$] below.

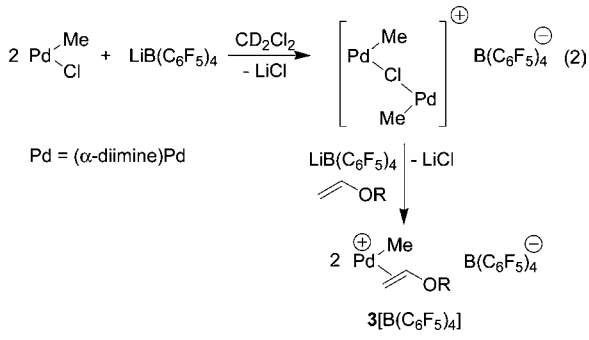

Cationic Polymerization of Vinyl Ethers by 1[$B(C_6F_5)_4$] and 1[SbF_6]. We first studied the reactions of **1**[$B(C_6F_5)_4$] with excess CH_2═CHOR (**2a**−**g**) to probe trends in cationic polymerization reactivity. As shown in eq 3, the reaction of **1**[$B(C_6F_5)_4$] with excess **2a** at 20 °C results in rapid (5 min) and quantitative polymerization of **2a**. The NMR spectra of the −[CH_2CH(O^{t}Bu)]$_n$− polymer are essentially identical to those of −[CH_2CH(O^{t}Bu)]$_n$− generated by cationic initiators such as [Ph_3C][$B(C_6F_5)_4$] or [Li(Et_2O)$_{2.8}$][$B(C_6F_5)_4$] under the same conditions. These −[CH_2CH(O^{t}Bu)]$_n$− polymers are atactic (mm/mr/rr = 1:3:1) and contain methyl (−CH(O^{t}Bu)C*H*$_3$), aldehyde (−CH_2C(═O)*H*), and acetal (−C*H*(O^{t}Bu)$_2$) end groups and internal −CH═CH− units (ca. 3 mol %).[23] These features are characteristic of a cationic polymerization process.[10,11,23,24] Interestingly, rapid formation of Pd^0 was observed during the polymerization of **2a**. The reaction of **1**[$B(C_6F_5)_4$] with excess **2b** at 20 °C is similar.

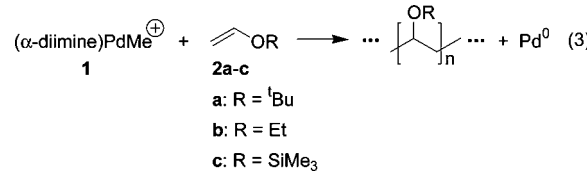

The reaction of **1**[$B(C_6F_5)_4$] with a large excess CH_2═CHOSiMe_3 (**2c**, 50 equiv, 1.2 M) in CD_2Cl_2 at 20 °C results in inefficient cationic polymerization to form −[CH_2CH(OSiMe_3)]$_n$− (7% conversion, 20 h). Pd^0 formation was also observed early in this reaction. However, when less than 10 equiv (0.25 M) of **2c** was used, no cationic polymerization was detected. In contrast, the reaction of **1**[$B(C_6F_5)_4$] with excess **2d**−**g** (ca. 80 equiv, 2.0 M) in CD_2Cl_2 at 20 °C does not generate polymer or Pd^0.[25] The reactions of **1**[SbF_6] with excess **2a**−**g** gave very similar results.

These results imply that the cationic polymerization and Pd^0 formation processes are closely related, and that both processes can be circumvented by using arylsilyl or aryl vinyl ethers.

Initiation of Cationic Polymerization of 2a−**c.** Two likely initiators for the cationic polymerization in eq 3 are the (α-diimine)PdMe$^+$ cation itself or H$^+$ generated from adventitious water (e.g., via formation of (α-diimine)PdMe(H_2O)$^+$). Bulky 2,6-disubstituted pyridines have been used as proton traps to quench the H$^+$-initiated cationic polymerization of vinyl ethers and other monomers.[11f,24b,26] Similarly, pyridine was shown to quench the cationic polymerization of vinyl ethers initiated by (P∼N)PdMe(H_2O)$^+$ species.[11b] However, control experiments show that 2,6-^{t}Bu$_2$-pyridine (DTBP) has only a minimal effect on the rate and yield of the **2a** polymerization in eq 3. This result suggests that (α-diimine)PdR′$^+$ (R′ = Me or CH_2CH(OR)Me formed by insertion, vide infra) species initiate this reaction.[27] A reasonable mechanism for the **1**-mediated polymerization of **2a**−**c** that accounts for these observations is

(22) Johnson, L. K.; Kilian, C. M.; Arthur, S. D.; Feldman, J.; Mccord, E. F.; Mclain, S. J.; Kreutzer, K. A.; Bennett, M. A.; Coughlin, E. B. PCT Int. Appl. WO 9623010, 1996.

(23) The−CH═CH−units are formed by elimination of HOR from the −[CH_2CH(OR)]$_n$−chain. See: Hashimoto, T.; Kanai, T.; Kodaira, T. *J. Polym. Sci., Part A: Polym. Chem.* **1998**, *36*, 675.

(24) (a) Wang, Q.; Baird, M. C. *Macromolecules* **1995**, *28*, 8021. (b) Kéki, S.; Nagy, M.; Deák, G.; Zsuga, M. *J. Phys. Chem. B* **2001**, *105*, 9896.

(25) When the in situ generated **1**[$B(C_6F_5)_4$] contains excess Li$B(C_6F_5)_4$, **2d** is slowly cationically polymerized. However, Pd^0 formation was not observed.

(26) (a) De, P.; Faust, R. *Macromolecules* **2006**, *39*, 7527. (b) Hadjikyriacou, S.; Acar, M.; Faust, R. *Macromolecules* **2004**, *37*, 7543. (c) Bennevault, W.; Peruch, F.; Defieux, A. *Macromol. Chem. Phys.* **1996**, *197*, 2603. (d) Cho, C. G.; Feit, B. A.; Webster, O. W. *Macromolecules* **1992**, *25*, 2081.

(27) (a) This result may also suggest that (α-diimine)PdMe(OH_2)$^+$ is too crowded to be deprotonated by DTBP. It was not possible to test the influence of pyridine on the **1**-initiated cationic polymerization since pyridine displaces the α-diimine ligand. (b) DTBP significantly retards the polymerization of **2a** by [Li(Et_2O)$_{2.8}$][$B(C_6F_5)_4$].

Scheme 3

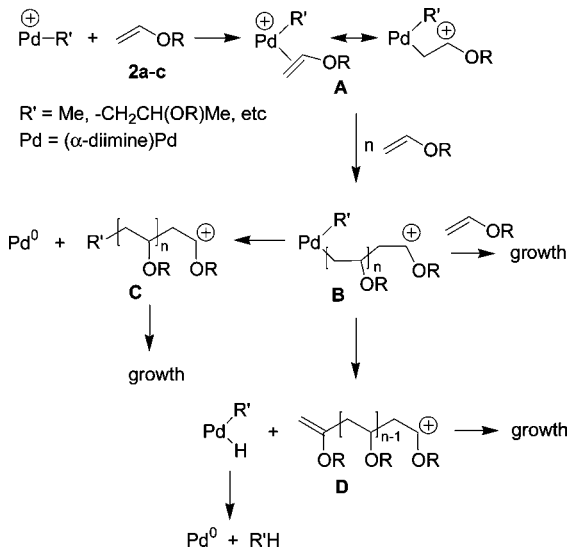

shown in Scheme 3. Coordination of the vinyl ether to a (α-diimine)PdR′$^+$ species generates an (α-diimine)-PdR′(CH$_2$=CHOR)$^+$ π complex (**A**), in which the vinyl ether C=C bond is polarized with carbocation character at the substituted carbon (C$_{int}$), due to the electrophilic character of the cationic Pd center.[15a,c] Electrophilic attack of C$_{int}$ of **A** on monomer then initiates cationic polymerization. Pd^0 formation can occur by reductive elimination of growing species **B** or more likely by β-H elimination of **B** followed by R′-H reductive elimination.[28,29]

Reaction of 1[SbF$_6$] or 1[B(C$_6$F$_5$)$_4$] with 1 Equiv of CH$_2$=CHOR (2a−g). Scheme 3 suggests that it might be possible to probe for vinyl ether insertion chemistry by generating (α-diimine)PdMe$^+$ species in the presence of stoichiometric quantities of vinyl ether, such that excess substrate is not present to propagate cationic polymerization. Indeed, as shown in the Scheme 4, reaction of **1**[SbF$_6$] or **1**[B(C$_6$F$_5$)$_4$] with 1 equiv of **2a**−**g** proceeds by initial formation of (α-diimine)PdMe(CH$_2$=CHOR)$^+$ (**3a**−**g**),[30] followed by 1,2 insertion to produce (α-diimine)Pd(CH$_2$CHMeOR)$^+$ (**4a**−**g**) and reversible isomerization to form (α-diimine)Pd(CMe$_2$OR)$^+$ (**5a**−**g**). The **4a**−**g**/**5a**−**g** mixtures react further at 20 °C by β-OR elimination of **4a**−**g** to generate (α-diimine)Pd-(OR)(CH$_2$=CHMe)$^+$ (not observed), followed by allylic C−H activation to yield (α-diimine)Pd(η^3-C$_3$H$_5$)$^+$ (**6**) and ROH as the ultimate products. These reactions are discussed in detail in the following sections.

Generation of [(α-Diimine)PdMe(CH$_2$=CHOR)][SbF$_6$] (3a−g[SbF$_6$]). The reaction of **1**[SbF$_6$] and **2a**−**g** in CD$_2$Cl$_2$ at −60 °C generates the corresponding adducts [(α-diimine)PdMe(CH$_2$=CHOR)][SbF$_6$] (**3a**−**g**[SbF$_6$]) in >90% yield.[31] No broadening of the ^{1}H NMR resonances of **3a**−**g** was detected in the presence of excess vinyl ether over the temperature range of −60 to 20 °C, and no EXSY cross peaks between the free and coordinated vinyl ether resonances were observed at −60 or −20 °C. These results show that the exchange between the free and coordinated vinyl ether is slow.

Scheme 4

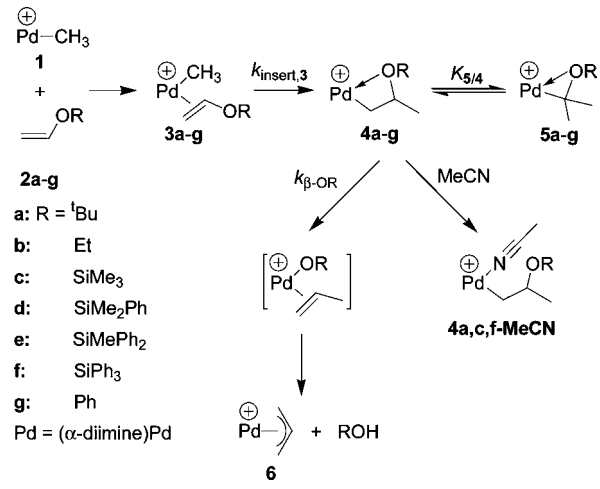

Table 1. ^{1}H and ^{13}C NMR Chemical Shifts for Free CH$_2$=CHO^{t}Bu (**2a**) and **3a**[SbF$_6$] (CD$_2$Cl$_2$, −60° C)

CH$_2$=CHO^{t}Bu	chemical shift (δ)		
resonance	free	coord	Δ^a
H$_{int}$	6.47	7.09	−0.62
H$_{trans}$	4.22	3.27	0.95
H$_{cis}$	3.93	2.96	0.97
C(C***H***$_3$)$_3$	1.21	1.35	−0.14
CH$_2$	90.4	54.4	36.0
CH	147.1	148.2	−1.1
C(CH$_3$)$_3$	76.4	83.6	−7.2

^{a} $\Delta = \delta_{free} - \delta_{coord}$.

Key NMR data for the *tert*-butyl vinyl ether complex **3a**[SbF$_6$] are listed in Table 1. The CH$_2$=C***H***O^{t}Bu ^{1}H resonance is shifted downfield and the C***H***$_2$=CHO^{t}Bu resonances are shifted upfield from the corresponding resonances of free CH$_2$=CHO^{t}Bu. Furthermore, the ***C***H$_2$=CHO^{t}Bu ^{13}C resonance is shifted significantly upfield, while the O***C***Me$_3$ resonance is shifted only slightly upon coordination. These data are characteristic for C=C-bound π complexes, such as CpFe(CO)$_2$-(CH$_2$=CHOEt)$^+$ and Cp′$_2$Zr(O^{t}Bu)(η^2-H$_2$C=CHO^{t}Bu)$^+$.[15a,c] In contrast, for O-coordinated CH$_2$=CHOR adducts, such as (C$_5$H$_4$Me)$_2$Zr(O^{t}Bu)(η^1-*O*-EtOCH=CH$_2$)$^+$ and RuH(CO)(P^{t}Bu$_2$Me)$_2$-(η^1-*O*-EtOCH=CH$_2$)$^+$, the H$_{trans}$ and H$_{cis}$ ^{1}H NMR resonances are shifted downfield, and the ***C***H$_2$=CHOEt and CH$_2$=CHO***C***H$_2$Me ^{13}C NMR resonances are shifted significantly upfield from those of free vinyl ether.[15c,16] The NMR spectra of **3b**−**g**[SbF$_6$] are similar to those of **3a**[SbF$_6$], showing that these species are also C=C π complexes.

The in situ generated (α-diimine)PdMe$^+$ system **1**[B(C$_6$F$_5$)$_4$] is less useful for the observation of **3**[B(C$_6$F$_5$)$_4$] complexes because displacement of (α-diimine)PdMeCl from the intermediate [{(α-diimine)PdMe}$_2$(μ-Cl)]$^+$ cation (eq 2) by vinyl ethers is slow. **1**[B(C$_6$F$_5$)$_4$] does not react with **2a** in CD$_2$Cl$_2$ at −60 °C, indicating that under these conditions the vinyl ether does not break the chloride bridge. However, when the [{(α-diimine)PdMe}$_2$(μ-Cl)]$^+$/[Li(Et$_2$O)$_{2.8}$][B(C$_6$F$_5$)$_4$]/**2a** mixture is warmed to 20 °C for 10 min, [(α-diimine)PdMe(CH$_2$=CHO^{t}Bu)][B(C$_6$F$_5$)$_4$] (**3a**[B(C$_6$F$_5$)$_4$]) is formed in 78% yield. The

(28) The end groups in species **C** and **D** were not detected by NMR, possibly because their NMR resonances overlap with, and are much weaker than, those of other end groups generated by chain transfer, which is fast (ca. 46−[CH$_2$CH(O^{t}Bu)]$_n$−chains are produced per Pd). The end group **D** may be incorporated into the polymer.

(29) (α-Diimine)PdR$_2$ complexes (R = ^{n}Pr, ^{n}Bu, ^{i}Bu) are moderately stable at room temperature. These species slowly decompose (days) to alkanes, alkenes, and unidentified Pd(0) species. See ref 2b.

(30) If the anion is not specified for complexes **3**, **4**, and **5**, the statement is true for both the SbF$_6^-$ and B(C$_6$F$_5$)$_4^-$ salts.

(31) The major impurity is [{(α-diimine)PdMe}$_2$(μ-Cl)][SbF$_6$].

Table 2. Reactivity of CH_2=CHOR with **1**[SbF_6][a]

CH_2=CHOR (**2**), R =	^{t}Bu (**2a**)	Et (**2b**)	$SiMe_3$ (**2c**)	$SiMe_2Ph$ (**2d**)	$SiMePh_2$ (**2e**)	$SiPh_3$ (**2f**)	Ph (**2g**)
$K_{2/ethylene}$ (−60 °C)[b]	0.88(2)	0.22(1)	0.12(1)				
$K_{2/2c}$ (−20 °C)[c]	5.35[d]	1.66[d]	1	0.34(4)	0.19(2)	0.08(1)	0.30(2)
$\Delta G_{2/2c}$ (kcal/mol, −20 °C)[e]	−0.8(1)	−0.2(1)	0	0.5(1)	0.8(1)	1.3(1)	0.6(1)
$k_{insert,3}$ (10^{-4} s^{-1}, 0 °C)	0.33(2)	0.84(5)	1.6 (1)	3.2(2)	5.2(3)	8.1(5)	15.0(9)
$k_{insert,3}$ (10^{-4} s^{-1}, 20 °C)	6.3(4)	~27	>33[f]	>33[f]	>33[f]	>33[f]	>33[f]
$\Delta G^{\ddagger}_{insert,3}$ (kcal/mol, 0 °C)[g]	21.5(1)	21.0(1)	20.7(1)	20.3(1)	20.0(1)	19.8(1)	19.4(1)
$K_{5/4}$ (0 °C)[h]	0.21	2.2	>19[i]	>19[i]	>19[i]	>19[i]	unknown[j]
$K_{5/4}$ (20 °C)[h]	0.33	2.7	>19[i]	>19[i]	>19[i]	>19[i]	unknown[j]
$k_{\beta\text{-OR,obs}}$ (10^{-6} s^{-1}, 20 °C)[k]	15.0(9)	1200(70)	111(7)	156(9)	246(15)	378(23)	>5000[l]
$k_{\beta\text{-OR}}$ (10^{-6} s^{-1}, 20 °C)[m]	20(1)	4440(260)	>2220[n]	>3120[n]	>4920[n]	>7560[n]	>5000[n]

[a] The uncertainties are based on replicate runs. [b] $K_{2/ethylene}$ = [**3**][CH_2=CH_2][(α-diimine)PdMe(CH_2=CH_2)$^+$]$^{-1}$[**2**]$^{-1}$ at equilibrium. [c] $K_{2/2c}$ = [**3**][**2c**][**3c**]$^{-1}$[**2**]$^{-1}$ at equilibrium. [d] ΔS of equilibrium is assumed to be negligible, so ΔG does not change over temperature.[33] $K_{2a,b/ethylene}$(−20 °C) = exp{(213/253)ln[$K_{2a,b/ethylene}$(−60 °C)]}; $K_{2a,b/2c}$ = $K_{2a,b/ethylene}$/$K_{2c/ethylene}$. [e] $\Delta G_{2/2c}$ = −RTln$K_{2/2c}$. [f] More than 95% of **3** undergoes insertion within 15 min at 20 °C. [g] The insertion barrier for **3a**−**g** at 0 °C, $\Delta G^{\ddagger}_{insert,3}$ = −RTln($k_{insert,3}$h/k_BT). [h] $K_{5/4}$ = [**5**]/[**4**] at equilibrium. [i] Complexes **4c**−**f** were not detected by NMR. [j] **4g** and **5g** were not observed due to fast β-OR elimination of **4g**. [k] The observed first-order rate constant for consumption of the total of **4** and **5**. [l] More than 95% of **3g** is converted to **6** and phenol within 10 min at 20 °C. [m] The first-order rate constant for β-OR elimination of **4**, $k_{\beta\text{-OR}}$ = $k_{\beta\text{-OR,obs}}$ ($K_{5/4}$ + 1). [n] Lower limit assuming $K_{5/4}$ > 20.

remaining species in solution are [{(α-diimine)PdMe}$_2$(μ-Cl)]$^+$ (8%) and the insertion products **4a**[$B(C_6F_5)_4$] (10%) and **5a**[$B(C_6F_5)_4$] (4%, Scheme 4). Complex **3b**[$B(C_6F_5)_4$] is formed in 27% yield by the reaction of **1**[$B(C_6F_5)_4$] and **2b** in CD_2Cl_2 at 20 °C for 10 min. The remaining species in solution are [{(α-diimine)PdMe}$_2$(μ-Cl)]$^+$ (8%), the insertion products **4b**[$B(C_6F_5)_4$] (18%) and **5b**[$B(C_6F_5)_4$] (35%), and allyl complex **6** (12%). Complexes **3c**−**g**[$B(C_6F_5)_4$] are not observed in the reaction of **1**[$B(C_6F_5)_4$] and **2c**−**g** at 20 °C due to fast insertion.

Two rotamers are possible for a (α-diimine)PdMe(CH_2=CHOR)$^+$ species, which differ in the orientation of the vinyl ether (eq 4). The ^{1}H NMR spectra of **3a**−**g** contain one set of sharp α-diimine, Pd−Me, and vinyl ether resonances over the temperature range of −70 to 20 °C (0 °C for **3g**; insertion is rapid above this temperature), suggesting that either rotation around the Pd−vinyl ether bond is very fast or, more likely, one rotamer is highly favored. NOSEY spectra of **3c**−**f** contain Pd−Me/CHMe_2, H_{cis}/CHMe_2, and H_{int}/CHMe_2′ cross peaks but no cross peaks between the Pd−Me and H_{int} or H_{cis} resonances. These results are consistent with a structure in which the C=C bond is oriented perpendicular to the N−N−Pd−Me square plane and the OR group points toward the Pd−Me group (endo rotamer).[32]

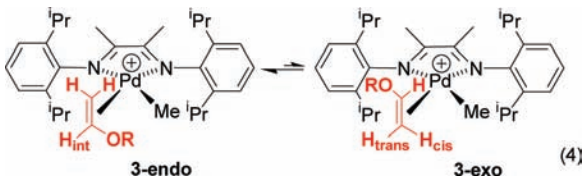

(4)

To further understand the structures and dynamics of these complexes, two less crowded examples, [{(2,6-^{i}Pr$_2$−C$_6$H$_3$)N=CAnCAn=N(2,6-^{i}Pr$_2$−C$_6$H$_3$)}PdMe(CH_2=CHOSiPh$_3$)][SbF_6] (**3h**, An,An = acenaphthyl) and [{(4-Me-C_6H_5)N=CMeCMe=N(4-Me-C_6H_5)}PdMe(CH_2=CHOSiPh$_3$)][SbF_6] (**3i**) were prepared. **3h** is similar to **3c**−**f** and exists as the endo isomer. However, at −70 °C in CD_2Cl_2, **3i** exists as a 1/1 mixture of endo and exo rotamers, which were identified by NOSEY correlations. The barrier for olefin rotation (i.e., interconversion of the endo and exo isomers) of **3i** ($\Delta G^{\ddagger}_{rotation}$ = 10.3 kcal/mol, −50 °C) was determined from the coalescence of the Pd−Me resonances.

Competitive Binding of Ethylene and Vinyl Ethers to 1. The relative binding strengths of vinyl ethers **2a**−**c** to **1**[SbF_6] were determined by competition experiments with ethylene (eq 5). The reactions of **1**[SbF_6] with excess ethylene and **2a**−**c** were monitored by ^{1}H NMR at −60 °C until the reaction quotient Q = [**3**][CH_2=CH_2][(α-diimine)PdMe(CH_2=CH_2)$^+$]$^{-1}$[**2**]$^{-1}$ reached a constant value ($K_{2/ethylene}$), indicating that the equilibrium in eq 5 had been reached. **2d**−**g** bind to Pd much more weakly than ethylene does, so their binding affinities cannot be measured accurately by eq 5. The binding affinities of **2d**−**g** were determined by competition experiments with **2c** (eq 6). These experiments were conducted at −20 °C in order to accelerate the approach to equilibrium. Equilibrium constants for eq 5 and 6 are listed in Table 2. The reactions of [(α-diimine)PdMe(CH_2=CH_2)][$B(C_6F_5)_4$] (generated in situ)[2d] with excess ethylene and **2a**−**c** gave very similar equilibrium constants (Table 3), showing that the counteranion (SbF_6^- vs $B(C_6F_5)_4^-$) does not strongly influence the relative binding ability of these substrates to **1**.

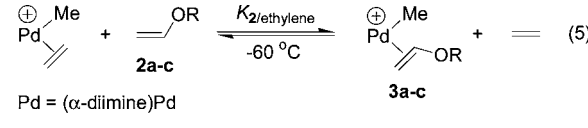

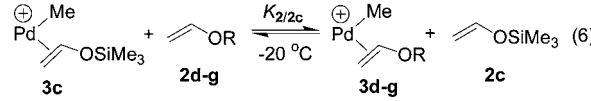

Insertion of [(α-Diimine)PdMe(CH_2=CHO^{t}Bu)][$B(C_6F_5)_4$] (3a[$B(C_6F_5)_4$]). The ^{t}Bu vinyl ether adduct **3a**[$B(C_6F_5)_4$] reacts to form [(α-diimine)Pd{CH_2CHMe(O^{t}Bu)}][$B(C_6F_5)_4$] (**4a**[$B(C_6F_5)_4$], 66%) and [(α-diimine)Pd{CMe_2(O^{t}Bu)}][$B(C_6F_5)_4$] (**5a**[$B(C_6F_5)_4$], 25%) in 2 h at 20 °C (Scheme 4). The first-order rate constant for the consumption of **3a**[$B(C_6F_5)_4$] was measured by ^{1}H NMR at 0

(32) (a) Two rotamers of [{(2,6-Me_2-C_6H_3)N=CAnCAn=N(2,6-Me_2-C_6H_3)}PdMe(η^2-CH_2=CHO_2CCH_3)}$^+$ were observed. See ref 6. (b) (Me_2bipy)PdMe(η^2-CH_2=CHCl)$^+$ (Me_2bipy = 4,4′-Me_2-2,2′-bipyridine) prefers the exo structure. See ref 7a.

(33) (a) This assumption was made by Brookhart and by Guan in studies of competitive binding of ethylene and methyl acrylate to (α-diimine)PdR$^+$ species. (b) Mecking, S.; Johnson, L. K.; Wang, L.; Brookhart, M. *J. Am. Chem. Soc.* **1998**, *120*, 888. (c) Popeney, C. S.; Guan, Z. B. *J. Am. Chem. Soc.* **2009**, *131*, 12384.

Table 3. Reactivity of CH_2=CHOR with **1**[$B(C_6F_5)_4$][a]

CH_2=CHOR (**2**), R =	^{t}Bu (**2a**)	Et (**2b**)	$SiMe_3$ (**2c**)	$SiMe_2Ph$ (**2d**)	$SiMePh_2$ (**2e**)	$SiPh_3$ (**2f**)	Ph (**2g**)
$K_{2/ethylene}$ (−60 °C)[b]	1.2(7)	0.21(1)	0.17(1)			<0.01	0.04(1)
$k_{insert,3}$ (10^{-4} s^{-1}, 0 °C)	0.33(2)	0.80(5)					
$k_{insert,3}$ (10^{-4} s^{-1}, 20 °C)	7.1(4)	~20	>33[c]	>33[c]	>33[c]	>33[c]	>33[c]
$K_{5/4}$ (0 °C)[d]	0.27	2.5	>19[e]	>19[e]	>19[e]	>19[e]	>19[e]
$K_{5/4}$ (20 °C)[d]	0.39	2.8	>19[e]	>19[e]	>19[e]	>19[e]	unknown[f]
$k_{\beta\text{-OR,obs}}$ (10^{-6} s^{-1}, 20 °C)[g]	2.3(1)	912(55)	32(2)	51(3)	134(8)	107(6)	>5000[h]
$k_{\beta\text{-OR}}$ (10^{-6} s^{-1}, 20 °C)[i]	3.2(2)	3460(200)	>640[j]	>1020[j]	>2680[j]	>2140[j]	>5000[j]

[a] The uncertainties are based on replicate runs. [b] $K_{2/ethylene}$ = [**3**][CH_2=CH_2][(α-diimine)PdMe(CH_2=CH_2)$^+$]$^{-1}$[**2**]$^{-1}$ at equilibrium. [c] More than 95% of **3** undergoes insertion within 15 min at 20 °C. [d] $K_{5/4}$ = [**5**]/[**4**] at equilibrium. [e] Complexes **4c**−**f** were not detected by NMR. [f] **4g** and **5g** were not observed due to fast β-OR elimination of **4g**. [g] The observed first-order rate constant for consumption of the total of **4** and **5**. [h] More than 95% of **3g** is converted to **6** and phenol within 10 min at 20 °C. [i] The first-order rate constant for β-OR elimination of **4**, $k_{\beta\text{-OR}} = k_{\beta\text{-OR,obs}}(K_{5/4} + 1)$. [j] Lower limit assuming $K_{5/4} > 20$.

and 20 °C (Table 3). For the alkyl ligand of **4a**[$B(C_6F_5)_4$], the ^{1}H and COSY NMR spectra contain a multiplet at δ 4.86 (CH), a doublet of doublets at δ 0.40 and a triplet at δ 0.93 (CH_2), and a doublet at δ 1.15 (CH_3). For the alkyl ligand of **5a**[$B(C_6F_5)_4$], the ^{1}H NMR spectrum comprises a singlet at δ 0.64. NMR data show that both **4a**[$B(C_6F_5)_4$] and **5a**[$B(C_6F_5)_4$] contain unsymmetrical α-diimine ligands, indicating that these species are four-coordinate rather than three-coordinate complexes. To probe for O-chelation in **4a** and **5a**, the reaction with CH_3CN was investigated. As shown in Scheme 4, the **4a**[$B(C_6F_5)_4$]/**5a**[$B(C_6F_5)_4$] mixture reacts with MeCN in CD_2Cl_2 at −40 °C to produce a single product, (α-diimine)Pd{$CH_2CHMe(O^tBu)$}$(NCMe)^+$ ([**4a**-MeCN][$B(C_6F_5)_4$]), quantitatively. The $PdCH_2\mathbf{\mathit{C}}H(O^tBu)Me$ (δ 67.2) and $PdCH_2CH(O\mathbf{\mathit{C}}Me_3)Me$ (δ 72.8) ^{13}C NMR resonances of [**4a**-MeCN][$B(C_6F_5)_4$] appear in the normal range for ^{i}Pr and ^{t}Bu ethers.[34] In contrast, the $PdCH_2\mathbf{\mathit{C}}H(O^tBu)Me$ (δ 88.3) and $PdCH_2CH(O\mathbf{\mathit{C}}Me_3)Me$ (δ 88.9) ^{13}C resonances of **4a**[$B(C_6F_5)_4$] and the $Pd\mathbf{\mathit{C}}Me_2(O^tBu)$ (δ 82.8) and $PdCMe_2(O\mathbf{\mathit{C}}Me_3)$ (δ 90.3) resonances of **5a**[$B(C_6F_5)_4$] are shifted far downfield from this range, indicating the presence of O-chelation in these species.[35−38]

Interconversion of 4a[$B(C_6F_5)_4$] and 5a[$B(C_6F_5)_4$]. The **5a**[$B(C_6F_5)_4$]/**4a**[$B(C_6F_5)_4$] ratio remains constant (0.39) during the formation of these species from **3a**[$B(C_6F_5)_4$] at 20 °C and their subsequent conversion to **6** at 20 °C (Scheme 4). These results imply that **4a**[$B(C_6F_5)_4$] and **5a**[$B(C_6F_5)_4$] interconvert rapidly on the laboratory time scale but slowly on the NMR chemical shift time scale at this temperature. NMR monitoring studies reveal that, during the reaction of **4a**[$B(C_6F_5)_4$]/**5a**[$B(C_6F_5)_4$] with MeCN (1.2 equiv), **4a**[$B(C_6F_5)_4$] is converted to [**4a**-MeCN][$B(C_6F_5)_4$] rapidly (within 5 min at −60 °C), while **5a**[$B(C_6F_5)_4$] is converted to [**4a**-MeCN][$B(C_6F_5)_4$] slowly (ca. 140 min at −40 °C). The adduct [**5a**-MeCN][$B(C_6F_5)_4$] was not detected. Therefore, at this temperature, **5a**[$B(C_6F_5)_4$] slowly rearranges to **4a**[$B(C_6F_5)_4$], which is then rapidly trapped by MeCN (Scheme 4).

Scheme 5

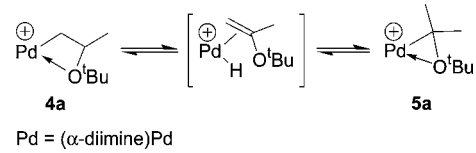

The interconversion of **4a**[$B(C_6F_5)_4$] and **5a**[$B(C_6F_5)_4$] occurs by a normal chain-walking mechanism, that is, β-H elimination to generate (α-diimine)$PdH(CH_2$=$CMe(O^tBu))^+$ (not observed) followed by re-insertion (Scheme 5). DFT studies show that the energy difference between **4a**[$B(C_6F_5)_4$] and **5a**[$B(C_6F_5)_4$] is small ($E_{4a} - E_{5a} = 0.2 \pm 1.0$ kcal/mol), which is consistent with the fact that both isomers are observed.

Conversion of 4a[$B(C_6F_5)_4$] and 5a[$B(C_6F_5)_4$] to (α-Diimine)Pd(η^3-C_3H_5)[$B(C_6F_5)_4$] (6[$B(C_6F_5)_4$]). The **4a**[$B(C_6F_5)_4$]/**5a**[$B(C_6F_5)_4$] mixture reacts to produce (α-diimine)Pd(η^3-C_3H_5)[$B(C_6F_5)_4$] (**6**[$B(C_6F_5)_4$]) and ^{t}BuOH quantitatively over the course of 15 days at 20 °C in CD_2Cl_2 solution (Scheme 4). Compound **6**[$B(C_6F_5)_4$] was prepared independently and fully characterized.

The most likely mechanism for the conversion of **4a**[$B(C_6F_5)_4$]/**5a**[$B(C_6F_5)_4$] to **6**[$B(C_6F_5)_4$] is β-OR elimination of **4a**[$B(C_6F_5)_4$] to generate (α-diimine)Pd(OR)(CH_2=$CHMe)^+$ (not observed), followed by allylic C−H activation (Scheme 4). Similar C−H activation reactions to form allyl species were reported by Bercaw for α-diimine Pt and Pd hydroxide complexes.[39] In related work, Hosokawa showed that in situ generated ClPd(OH)(propene) undergoes allylic C−H activation to form {(π-allyl)PdCl}$_2$ and H_2O.[40] Also, the reaction of Pd(II) chloride salts with α-olefins to generate (π-allyl)Pd(II) complexes is well-known.[41]

As noted above, the **5a**[$B(C_6F_5)_4$]/**4a**[$B(C_6F_5)_4$] ratio remains constant during the conversion of **4a**[$B(C_6F_5)_4$]/**5a**[$B(C_6F_5)_4$] to **6**[$B(C_6F_5)_4$], indicating that the **4a**[$B(C_6F_5)_4$]/**5a**[$B(C_6F_5)_4$] exchange is faster than the β-O^{t}Bu elimination of **4a**[$B(C_6F_5)_4$].

(34) ^{13}C NMR ($CDCl_3$): $Me_2\mathbf{\mathit{C}}HOCMe_3$, δ 63.4; Me_2CHO $\mathbf{\mathit{C}}Me_3$, δ 72.7.

(35) The possible coordination of the excess CH_2=CHO^{t}Bu or Et_2O present in solution was ruled out because NMR data show that these species are free. After removal of volatiles from the mixture, the NMR resonances for **4a** and **5a** are unchanged, confirming that excess CH_2=CHO^{t}Bu and Et_2O do not bind to these species. β-H agostic interactions were not detected in **4a**[$B(C_6F_5)_4$] and **5a**[$B(C_6F_5)_4$] by ultra-low-temperature NMR ($CDCl_2F$ solution, −130 °C). Under similar conditions ($CDCl_2F$, −120 °C), the ^{1}H NMR resonance for the agostic H in (α-diimine)Pd{$CH(CH_2$-μ-$\mathbf{\mathit{H}})CH_3$}$^+$ (δ −7.85) was observed. See ref 2d.

(36) For comparison, the $O(\mathbf{\mathit{C}}H_2CH_3)_2$ 13C NMR resonance for (α-diimine)$PdMe(OEt_2)^+$ appears at δ 71.5, while the corresponding resonance for free $O(\mathbf{\mathit{C}}H_2CH_3)_2$ appears at δ 65.7. See ref 2e.

(37) O-Chelation in the analogous species Ru(η^2-$CH_2CH_2OCH_3$)(CO)(P^tBu_2Me)$_2^+$ was established by X-ray diffraction. The $RuCH_2\mathbf{\mathit{C}}H_2OCH_3$ and $RuCH_2CH_2O\mathbf{\mathit{C}}H_3$ ^{13}C NMR resonances occur at δ 89.6 and 60.6 ppm, respectively. See ref 16.

(38) DFT calculations confirmed that **4** and **5** have O-chelated structures. See the Supporting Information.

(39) (a) Driver, T. G.; Williams, T. J.; Labinger, J. A.; Bercaw, J. E. *Organometallics* **2007**, *26*, 294. (b) Bercaw, J. E.; Hazari, N.; Labinger, J. A.; Oblad, P. F. *Angew. Chem., Int. Ed.* **2008**, *47*, 9941. (c) Williams, T. J.; Caffyn, A. J. M.; Hazari, N.; Oblad, P. F.; Labinger, J. A.; Bercaw, J. E. *J. Am. Chem. Soc.* **2008**, *130*, 2418.

(40) Hosokawa, T.; Tsuji, T.; Mizumoto, Y.; Murahashi, S. I. *J. Organomet. Chem.* **1999**, *574*, 99.

(41) (a) Morellir, D.; Ugo, R.; Conti, F.; Donati, M. *Chem. Commun.* **1967**, *16*, 801. (b) Ketley, A. D.; Braatz, J. *Chem. Commun.* **1968**, *3*, 169.

Scheme 6

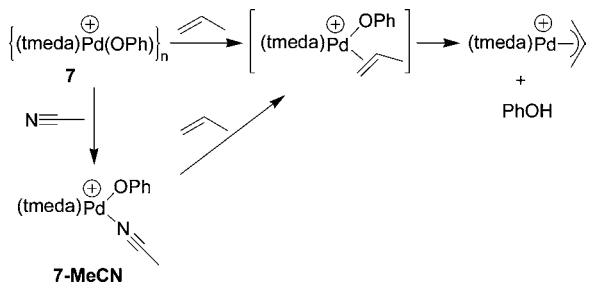

Therefore, the conversion of **4a**[$B(C_6F_5)_4$]/**5a**[$B(C_6F_5)_4$] to **6**[$B(C_6F_5)_4$] obeys pre-equilibrium kinetics. The observed first-order rate constant $k_{\beta\text{-O}^t\text{Bu,obs}}$ for consumption of the total of **4a**[$B(C_6F_5)_4$] and **5a**[$B(C_6F_5)_4$] and the formation of **6**[$B(C_6F_5)_4$] was measured by ^{1}H NMR. The first-order rate constant for β-O^{t}Bu elimination ($k_{\beta\text{-O}^t\text{Bu}}$) of **4a**[$B(C_6F_5)_4$] is given by eq 7.[42] Values for these rate constants are listed in Table 3.

$$k_{\beta\text{-O}^t\text{Bu}} = k_{\beta\text{-O}^t\text{Bu,obs}}(K_{\mathbf{5a/4a}} + 1) \quad (7)$$

Model Allylic C−H Activation Reaction. Attempts to prepare discrete (α-diimine)Pd(OR)$^+$ species to probe if they react with propene by allylic C−H activation as proposed in Scheme 4 were unsuccessful. However, the model compound [{(tmeda)Pd(OPh)}$_n$][$B(C_6F_5)_4$]$_n$ (**7**, tmeda = *N*,*N*,*N*′,*N*′-tetramethyl ethylenediamine) was generated in situ by the reaction of (tmeda)Pd(OPh)$_2$[43] with [$HNMe_2Ph$][$B(C_6F_5)_4$]. The base-free species **7** is believed to be a labile oligomer in solution (see Experimental Section). Complex **7** reacts with MeCN to generate the monomeric species [(tmeda)Pd(OPh)(NCMe)][$B(C_6F_5)_4$] (**7**-MeCN). Both **7** and **7**-MeCN react with propylene to produce [(tmeda)Pd(η^3-C_3H_5)][$B(C_6F_5)_4$] and phenol at 20 °C (Scheme 6). The propylene complex [(tmeda)Pd(OPh)(CH_2═CHMe)][$B(C_6F_5)_4$] was not detected by NMR monitoring of these reactions, which suggests that the allylic C−H activation step is facile.

Reaction of 1[SbF_6] with 2a. The reaction of **1**[SbF_6] with **2a** is similar to that of **1**[$B(C_6F_5)_4$] with **2a**, and the NMR data for **5a**[SbF_6]/**4a**[SbF_6] are very similar to those for **5a**[$B(C_6F_5)_4$]/**4a**[$B(C_6F_5)_4$]. The insertion rate constant ($k_{\text{insert,3a}}$) and equilibrium constant ($K_{\mathbf{5a/4a}}$) are also very similar for both cases (Table 2). However, the β-OR elimination rate constant of **4a**[SbF_6] ($k_{\beta\text{-OR}}$) is 6.5 times greater than that of **4a**[$B(C_6F_5)_4$] (Tables 2 and 3).

Reactions of 1[$B(C_6F_5)_4$] and 1[SbF_6] with 2b−g. The key features of these reactions that are different from the reactions of **2a** are summarized in this section, and key equilibrium and rate constants are given in Tables 2 and 3. Ethyl vinyl ether (**2b**) binds less strongly than **1**[$B(C_6F_5)_4$] but inserts more rapidly compared to **2a**. Interestingly, while $K_{\mathbf{5b/4b}}$ is greater than $K_{\mathbf{5a/4a}}$, β-OEt elimination of **4b** is 10^3 faster than β-O^{t}Bu elimination of **4a**. Similar results are observed for the reaction of **1**[SbF_6] with **2b**. The insertion rate constant ($k_{\text{insert,3b}}$) and equilibrium constant ($K_{\mathbf{5b/4b}}$) are very similar for both the [$B(C_6F_5)_4$]$^-$ and [SbF_6]$^-$ anions, while the β-OR elimination rate constant of **4b**[SbF_6] ($k_{\beta\text{-OR}}$) is 1.3 times greater than that of **4b**[$B(C_6F_5)_4$].

The reactions of **1**[SbF_6] with **2c**−**g** are similar to those with **2a**. The insertion rate constant $k_{\text{insert,3}}$ of the silyl vinyl ether complexes at 0 °C follows the order **3f** > **3e** > **3d** > **3c**. However, the formation of **3c**−**f**[$B(C_6F_5)_4$] from the reaction of **1**[$B(C_6F_5)_4$] with **2c**−**f** is slower than the subsequent insertion reactions, so accurate $k_{\text{insert,3}}$ values could not be obtained in these cases.

The direct insertion products **4c**−**f** were not detected by NMR, which implies that $K_{\mathbf{5c-f/4c-f}} > 19$. DFT studies show that both **4c** and **5c** have O-chelated structures and that **5c** is 3.6 ± 1 kcal/mol more stable than **4c**, consistent with the fact that only **5c** is observed. **5c,f**[$B(C_6F_5)_4$] react with MeCN to afford [**4c,f**-MeCN][$B(C_6F_5)_4$] in >90% yield, which confirms that **4c,f**[$B(C_6F_5)_4$] and **5c,f**[$B(C_6F_5)_4$] readily interconvert.

Complexes **5c**−**f** react to generate **6** (100%) and ROH via rearrangement to **4c**−**f** followed by β-OR elimination and allylic C−H activation. In the case of **5c**,**d**, the ROH products react further to yield R_2O and H_2O. The observed β-OR elimination rate constant ($k_{\beta\text{-OR,obs}}$) follows the order **f** > **e** > **d** > **c**. As observed for **2a**,**b**, the observed β-OR elimination rate constant of **4c**−**f**/**5c**−**f**[SbF_6] ($k_{\beta\text{-OR,obs}}$) is greater than that of **4c**−**f**/**5c**−**f**[$B(C_6F_5)_4$].

NMR monitoring studies of the reaction of phenyl vinyl ether complex **3g** ($B(C_6F_5)_4^-$ and SbF_6^- salts) at 0−20 °C reveal smooth quantitative conversion to **6** and phenol. Neither the 1,2 insertion product **4g** nor its chain-walk isomer **5g** was detected, which indicates that β-OPh elimination of **4g** is fast.[44]

Other α-Diimine Ligands. The insertion rate constant of sterically open **3h** ($k_{\text{insert}} = 2.0 \times 10^{-4}$ s^{-1} at 0 °C) is 4 times smaller than that of **3f** (8.1×10^{-4} s^{-1} at 0 °C). This difference is consistent with the trend observed in analogous ethylene insertion reactions.[2d,45] The β-$OSiPh_3$ elimination rate of [{(2,6-^{i}Pr$_2$−C_6H_3)N═CAnCAn═N(2,6-^{i}Pr$_2$−C_6H_3)}PdCMe$_2$($OSiPh_3$)][SbF_6] (**5h**) ($k_{\beta\text{-OSiPh}_3\text{,obs}} = 1.37\times 10^{-4}$ s^{-1} at 20 °C) is also slower that that of **5f** ($k_{\beta\text{-OSiPh}_3\text{,obs}} = 3.78 \times 10^{-4}$ s^{-1} at 20 °C). These results show that decreasing the steric crowding around the Pd center decreases the rate of both the CH_2═CHOSiPh_3 insertion and β-$OSiPh_3$ elimination reactions.

Discussion

The results described above provide insights into the cationic polymerization and insertion processes observed in the reactions of vinyl ethers with (α-diimine)PdMe$^+$ (**1**). First, the efficiency of **1**-initiated cationic polymerization varies in the order CH_2═CHO^{t}Bu (**2a**) > CH_2═CHOEt (**2b**) > CH_2═CHOSiMe_3 (**2c**), and this process is not observed for CH_2═CHOSiMe_2Ph (**2d**), CH_2═CHOSi$MePh_2$ (**2e**), CH_2═CHOSiPh_3 (**2f**), or CH_2═CHOPh (**2g**). The **1**-initiated cationic polymerization of **2a**,**b** and the corresponding Pd^0 formation preclude the use of these vinyl ethers as comonomers in olefin polymerization (Scheme 1).[20] The **1**-initiated cationic polymerization of **2c** is fast enough to compete with **1**-initiated 1-hexene/**2c** insertion copolymerization and renders this process inefficient.

The trend in the efficiency of **1**-initiated cationic polymerization rate, **2a** > **2b** > **2g**, is consistent with the classical trend for cationic polymerization by other initiators.[10−12,46] The key

(42) Wright, M. R. *An Introduction to Chemical Kinetics*; John Wiley & Sons: New York, 2004; p 346.
(43) Alsters, P. L.; Baesjou, P. J.; Janssen, M. D.; Kooijman, H.; Roetman, A. S.; Spek, A. L.; Koten, G. V. *Organometallics* **1992**, *11*, 4124.
(44) 2,6-Dimethylphenyl vinyl ether, 2-*tert*-butylphenyl vinyl ether, pentafluorophenyl vinyl ether, and 4-nitrophenyl vinyl ether react similarly to **2g**.
(45) Consistent with this trend, the insertion of **3i** ($k_{\text{insert,3i}} = 1.76 \times 10^{-4}$ s^{-1} at 0 °C) is slower than that of **3f** or **3h**. However, in this case, the insertion product is not stable and multiple species and Pd^0 are formed.
(46) (a) Aoki, S.; Stille, J. K. *Macromolecules* **1970**, *3*, 473. (b) Plesch, P. H.; Shamliam, S. H. *Eur. Polym. J.* **1990**, *26*, 1113. (c) Shildknecht, C. E.; Zoss, A. O.; Grosser, F. *Ind. Eng. Chem.* **1949**, *41*, 2891. (d) Matsumoto, H. J.; Okamura, S. *Kobunshi Kugaku* **1968**, *26*, 702.

Scheme 7

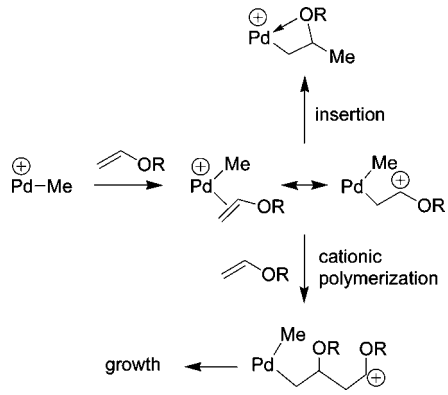

parameter that influences the reactivity of these substrates is the electron-donating ability of the OR group, which activates the C=C bond for electrophilic attack and stabilizes the growing alkoxycarbenium ion.[47] It is surprising that **2c**−**f** are not cationically polymerized by **1** since silyl vinyl ethers including **2c**,**d** are readily polymerized by Lewis acids such as $EtAlCl_2$, $SnCl_4$, $TiCl_4$, and BF_3.[48] Moreover, kinetic studies of the reactions of Ar_2CH^+ cations with vinyl ethers show that silyl vinyl ethers have similar or higher nucleophilicity compared to analogous alkyl vinyl ethers.[49] Also, we showed that $Ag[SbF_6]$, $[Li(OEt_2)_{2.8}][B(C_6F_5)_4]$, $[Ph_3C][B(C_6F_5)_4]$, and $[H(OEt_2)_2][B(C_6F_5)_4]$ initiate cationic polymerization of **2c**−**g** under the conditions studied here. The low efficiency (**2c**) or absence (**2d**−**f**) of cationic polymerization of **2c**−**f** by **1** is due to competing insertion chemistry, which consumes **1**. As noted above, **1**$[B(C_6F_5)_4]$ undergoes up to three sequential insertions of **2f**, ultimately forming Pd allyl products (Scheme 2).[21] Analogous multiple insertion reactions occur for **2c**−**f**. Similarly, it is surprising that **2g** is not cationically polymerized by **1** since other cationic initiators such as $[4\text{-}ClC_6H_4CO][SbF_6]$ and $SnCl_4$ readily polymerize this monomer.[50] In this case, fast insertion and β-OPh elimination out-compete cationic polymerization and produce (α-diimine)Pd(η^3-C_3H_5) (**6**) and PhOH (Scheme 1). The Pd allyl products of these reactions are not active for cationic polymerization.

The competition between cationic polymerization, which dominates for **2a**,**b**, and insertion chemistry, which dominates for **2d**−**g**, is controlled by the relative rates of these processes (Scheme 7). As noted above, literature data suggest that the inherent reactivity of alkyl and silyl vinyl ethers toward cationic polymerization is similar, which in turn suggests that the key factor that influences the competition between polymerization and insertion is the insertion rate constant of the (α-diimine)PdMe(CH_2=CHOR)$^+$ adduct ($k_{insert,3}$). The $k_{insert,3a,b}$ values are relatively small, so cationic polymerization dominates for **2a**,**b**. However, the $k_{insert,3d-g}$ values are more than 4 times larger than $k_{insert,3b}$, and thus insertion chemistry predominates for **2d**−**g**. The value for $k_{insert,3c}$ is only 2 times larger than $k_{insert,3b}$, and both insertion and cationic polymerization proceed for **2c**; the latter process is favored at higher **2c** concentrations because it is first-order in **2c**, while the insertion of **3c** is zero-order in **2c**.

It should be noted that, in some cases, cationic polymerization of silyl vinyl ethers is terminated or prevented by desilylation of the growing siloxy carbenium ion by nucleophilic attack at the SiR_3 group to yield oligomers or polymers with $-CH_2C(=O)R$ end groups. For example, Rimmer showed that the reaction of CH_2=CHO^{i}Bu and CH_2=CPh(OSiMe$_3$) with a HCl·CH_2=CHO^{i}Bu/$TiCl_4$ initiator system yields oligomers of general structure $H(CH_2CHO^iBu)_nCH_2C(=O)Ph$.[51] This reaction proceeds by cationic polymerization of CH_2=CHO^{i}Bu, occasional addition of the growing alkoxy carbenium ion to CH_2=CPh(OSiMe$_3$) to yield $H(CH_2CHO^iBu)_nCH_2CPh(OSiMe_3)^+$, and reaction with Cl^- to yield $H(CH_2CHO^iBu)_nCH_2C(=O)Ph$ and Me_3SiCl. Desilylations of this type can occur when Cl^- or F^- are present.[52] Several lines of evidence establish that the absence of cationic polymerization of **2d**−**f** by **1** is not due to such desilylation reactions. First, essentially quantitative yields of the Pd allyl products derived from multiple insertion, but no aldehyde products, are observed in the reaction of **1** with excess CH_2=CHSiPh$_3$ (**2f**, Scheme 2). Second, the relatively stable, poorly nucleophilic anions $[SbF_6]^-$ or $[B(C_6F_5)_4]^-$ are used as counterions for **1**. Third, as noted above, $Ag[SbF_6]$, $[Li(OEt_2)_{2.8}][B(C_6F_5)_4]$, $[Ph_3C][B(C_6F_5)_4]$, and $[H(OEt_2)_2][B(C_6F_5)_4]$ all initiate cationic polymerization of **2c**−**f** under the conditions studied here.[53]

Liu et al. reported that [(1-PPh$_2$-2-N=CHAr−C_6H_4)-PdMe(H_2O)][BF_4] (Ar = 4-FC_6H_4, C_6H_5) initiates fast cationic polymerization of alkyl vinyl ethers but not of CH_2=CHOSiMe$_3$.[11c] Our results suggest that insertion chemistry similar to that observed for (α-diimine)PdMe$^+$ may out-compete cationic polymerization in the latter case.

Under conditions where the cationic polymerization is circumvented, that is, by using low concentrations of **2a**−**c** or by using **2d**−**g**, the vinyl ether undergoes the C=C π coordination, insertion, chain-walking, β-OR elimination, and allylic C−H activation process shown in Scheme 4. The relative binding strengths of CH_2=CHOR vary in the order CH_2=CHO^{t}Bu (**2a**) > CH_2=CHOEt (**2b**) ∼ CH_2=CHOSiMe$_3$ (**2c**) > CH_2=CHOSiMe$_2$Ph (**2d**) ∼ CH_2=CHOPh (**2g**) > CH_2=CHOSiMePh$_2$ (**2e**) > CH_2=CHOSiPh$_3$ (**2f**). The binding strength trend reflects a combination of electronic and steric effects. The σ-donation component dominates the Pd−olefin bonding in (α-diimine)PdR(olefin)$^+$ species due to the poor

(47) (a) Yuki, H.; Hatada, K.; Nagata, K.; Emura, T. *Polym. J.* **1970**, *1*, 269. (b) Hatada, K.; Nagata, K.; Yuki, H. *Bull. Chem. Soc. Jpn.* **1970**, *43*, 3195. (c) Hatada, K.; Nagata, K.; Hasegawa, T.; Yuki, H. *Makromol. Chem.* **1977**, *178*, 2413. (d) Hatada, K.; Kitayama, T.; Nishiura, T.; Shibuya, W. *J. Polym. Sci., Part A* **2002**, *40*, 2134.

(48) (a) Murahashi, S.; Nozakura, S.; Sumi, M. *J. Polym. Sci., Part B* **1965**, *3*, 245. (b) Nozakura, S.; Ishihara, S.; Inaba, Y.; Matsumura, K.; Murahashi, S. *J. Polym. Sci.* **1973**, *11*, 1053. (c) Solaro, R.; Chiellini, E. *Gazz. Chim. Ital.* **1976**, *106*, 1037. (d) Palos, I.; Cadenas-Pliego, G.; Knjazhanski, S. Y.; Jimenez-Regalado, E. J.; Casas, E. G. D.; Ponce-Ibarra, V. H. *Polym. Degrad. Stab.* **2005**, *90*, 264.

(49) (a) Bartl, J.; Steenken, S.; Mayr, H. *J. Am. Chem. Soc.* **1991**, *113*, 7710. (b) Burfeindt, J.; Patz, M.; Muller, M.; Mayr, H. *J. Am. Chem. Soc.* **1998**, *120*, 3629.

(50) (a) Plesch, P. H.; Shamlian, S. H. *Eur. Polym. J.* **1990**, *26*, 1113. (b) Heublein, G.; Wondraczek, R. *Acta Polym.* **1980**, *31*, 558. (c) Yamamoto, K.; Higashimura, T. *Polymer* **1975**, *16*, 815.

(51) (a) Lang, W. H.; Sarker, P. K.; Rimmer, S. *Macromol. Chem. Phys.* **2004**, *205*, 1011. (b) Sarker, P. K.; Rimmer, S. *Macromol. Chem. Phys.* **2005**, *206*, 1280.

(52) (a) Sawamoto, M.; Okamoto, C.; Higashimura, T. *Macromolecules* **1987**, *20*, 2693. (b) Cramail, H.; Deffieux, A. *J. Phys. Org. Chem.* **1995**, *8*, 293. (c) Kuwajima, I.; Nakamura, E.; Shimizu, M. *J. Am. Chem. Soc.* **1982**, *104*, 1025. (d) Huffman, J. W.; Potnis, S. M.; Satish, A. V. *J. Org. Chem.* **1985**, *50*, 4266.

(53) It is highly unlikely that the LiCl that is generated as a byproduct in in situ activation of (α-diimine)PdMeCl with $[Li(OEt_2)_{2.8}][B(C_6F_5)_4]$ inhibits or prevents cationic polymerization of **2c**−**g** because LiCl is not soluble in CD_2Cl_2, and the discrete catalyst **1**$[SbF_6]$ does not initiate cationic polymerization of **2c**−**g**.

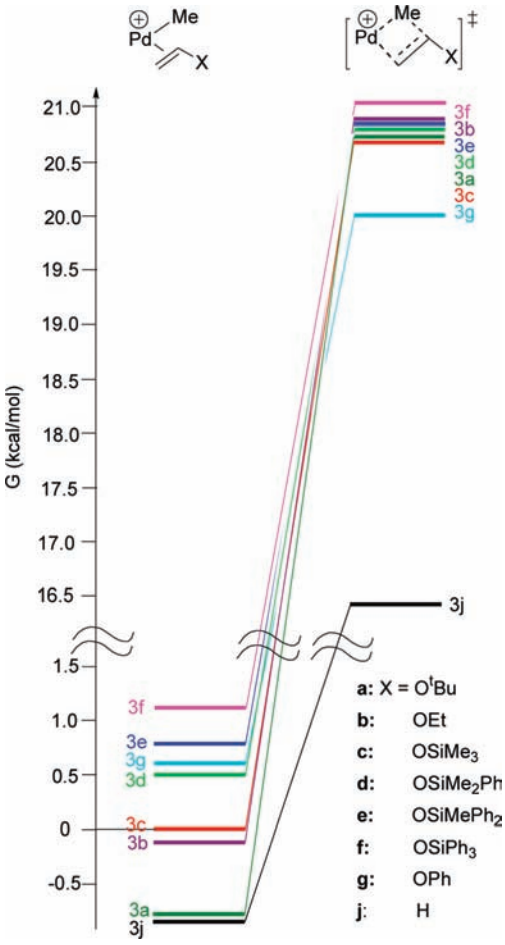

Figure 1. Energy diagram for insertion of **3a**−**g**[SbF_6]. Relative ground-state energies (versus **3c**) are based on $K_{2/ethylene}$ and $K_{2/2c}$ values in Table 2. Transition-state energies are based on $k_{insert,3}$ data in Table 2. $\Delta G^{\ddagger}$ for **3j** is based on the $k_{insert,ethylene}$ value in ref 2d.

back-bonding ability of the cationic Pd(II) center.[54] The trend in binding strengths, **2a** > **2c** > **2g**, parallels the trend in the DFT-calculated HOMO energies **2a** (−5.76 eV) > **2c** (−5.86 eV) > **2g** (−5.95 eV).[17,55] The DFT-calculated HOMO energies of **2c** and **2b** (−5.89 eV) are similar, but **2c** is more sterically bulky and hence binds more weakly compared to **2b**. The trend in binding strength **2c** > **2d** > **2e** > **2f** is expected because these substrates become poorer donors and more sterically crowded as methyl groups are replaced by phenyl groups.

The vinyl ether adducts **3a**−**g**[SbF_6] undergo insertion with exclusively 1,2 regioselectivity. The insertion rate constants ($k_{insert,3}$, Table 2) vary in the order **3a** < **3b** < **3c** < **3d** < **3e** < **3f** < **3g**. An energy diagram for the insertion of **3a**−**g** and (α-diimine)PdMe(ethylene)$^+$ based on ground-state energies (versus **3c**) derived from competitive binding studies ($K_{2/ethylene}$ and $K_{2/2c}$ in Table 2) and insertion barriers determined from insertion rate constants ($k_{insert,3}$, Table 2; $k_{insert,ethylene} = 900 \times 10^{-4}$ s^{-1} at 0 °C[2d]) is shown in Figure 1. The major factor contributing to the difference in the insertion barriers of **3a**−**g** is the ground-state energy of the vinyl ether adduct. As noted above, strongly electron-donating OR groups increase the binding strength and hence lower the ground-state energy and increase the insertion barrier, while steric crowding has the opposite effect.[2d] Complexes **3a**−**g** all insert more slowly than (α-diimine)PdMe(ethylene)$^+$.

The 1,2 insertion products (α-diimine)Pd{$CH_2CH(OR)Me$}$^+$ (**4a**−**f**) rapidly and reversibly isomerize to the chain-walk isomers (α-diimine)Pd{$CMe_2(OR)$}$^+$ (**5a**−**f**) via β-H elimination/reinsertion. The equilibrium constants $K_{5/4}$ increase in the order $K_{5a/4a} < K_{5b/4b} \ll K_{5c-f/4c-f}$ (only **5** is observed), showing that as the R group changes from alkyl to silyl the preference for **5** versus **4** increases. This trend may reflect the trend in electron-donating ability of the OR group O^{t}Bu > OEt > $OSiR_3$.[56] Previous studies have shown that L_nM-R bonds are strengthened by the presence of electron-withdrawing substitutents on C_α of the R group, which can stabilize the δ^- charge on C_α resulting from the inherent polarization of the M−C bond.[57] Electron-donating groups are expected to exert the opposite effect, so strongly electron-donating −OR groups exhibit small $K_{5/4}$ values. Steric factors may also influence $K_{5/4}$; however, this issue is difficult to assess since the relative steric crowding in **4** versus **5** will be sensitive to the identity of the OR group.

Complexes **4a**−**g** undergo β-OR elimination. The observed β-OR elimination rate constants for the **4**/**5** mixtures ($k_{\beta\text{-OR,obs}}$) vary in the order O^{t}Bu < $OSiR_3$ < OPh. This trend parallels the expected order of leaving group ability $^-$O^{t}Bu < $^-OSiR_3$ < $^-$OPh.[58] β-OR elimination is also more facile for small OR groups; for example, β-OEt elimination is much faster than β-O^{t}Bu elimination.[59] The fast β-OAr elimination of **4g** and analogous (α-diimine)PdCH_2CHOAr^+ species[44] precludes the use of aryl vinyl ethers as comonomers in **1**-catalyzed olefin polymerization (Scheme 1).

The data in Tables 2 and 3 show that the anion (SbF_6^- vs $B(C_6F_5)_4^-$) has only a small influence on the vinyl ether binding strength ($K_{2a-c/ethylene}$), the vinyl ether insertion rates ($k_{insert,3}$), or subsequent chain-walking ($K_{5/4}$). However, the $k_{\beta\text{-OR,obs}}$ values for **4a**−**f**[SbF_6]/**5a**−**f**[SbF_6] are 1.3 to 6.5 times greater than

(54) (a) Burns, C. T.; Jordan, R. F. *Organometallics* **2007**, *26*, 6726. (b) Burns, C. T.; Jordan, R. F. *Organometallics* **2007**, *26*, 6737. (c) Willner, H.; Aubke, F. *Organometallics* **2003**, *22*, 3612. (d) Lupinetti, A. J.; Strauss, S. H.; Frenking, G. *Prog. Inorg. Chem.* **2001**, *49*, 1. (e) Rix, F. C.; Brookhart, M. *J. Am. Chem. Soc.* **1995**, *117*, 1137. (f) Rix, F. C.; Brookhart, M.; White, P. S. *J. Am. Chem. Soc.* **1996**, *118*, 4746.

(55) (a) Kaëer, P.; Tobičik, J.; Kuzma, M.; Červený, L. *J. Mol. Catal. A* **2003**, *195*, 235.

(56) The electron-donating ability trend O^{t}Bu > OEt > $OSiR_3$ parallels the order of pK_a values of the conjugate acids HOR: HO^{t}Bu (17) > HOEt (15.9) > $HOSiMe_3$ (12.7) > $HOSiPh_3$ (10.8).

(57) (a) Axe, F. U.; Marynick, D. S. *J. Am. Chem. Soc.* **1988**, *110*, 3728. (b) Cotton, J. D.; Markwell, R. D. *J. Organomet. Chem.* **1990**, *388*, 123. (c) Cotton, J. D.; Crisp, G. T.; Daly, V. A. *Inorg. Chim. Acta* **1981**, *47*, 165. (d) Cross, R. J.; Gemmill, J. *J. Chem. Soc., Dalton Trans.* **1981**, 2317. (e) Cawse, J. N.; Fiato, R. A.; Pruett, R. L. *J. Organomet. Chem.* **1979**, *172*, 405. (f) Anderson, G. K.; Cross, R. *J. Acc. Chem. Res.* **1984**, *17*, 67. (g) Kuhlmann, E. J.; Alexander, J. J. *Coord. Chem. Rev.* **1980**, *33*, 195. (h) Calderazzo, F.; Noack, K. *Coord. Chem. Rev.* **1966**, *1*, 118. (i) Koga, N.; Morokuma, K. *J. Am. Chem. Soc.* **1986**, *108*, 6136. (j) Galamb, V.; Pályi, G.; Boese, R.; Schmid, G. *Organometallics* **1987**, *6*, 861. (k) Clot, E.; Besora, M.; Maseras, F.; Mégret, C.; Eisenstein, O.; Oelckers, B.; Perutz, R. N. *Chem. Commun.* **2003**, 490. (l) Clot, E.; Mégret, C.; Eisenstein, O.; Perutz, R. N. *J. Am. Chem. Soc.* **2009**, *131*, 7817. (m) Evans, M. E.; Burke, C. L.; Yaibuathes, S.; Clot, E.; Eisenstein, O.; Jones, W. D. *J. Am. Chem. Soc.* **2009**, *131*, 13464.

(58) As noted by Caulton, since β-OR elimination implies migration of the RO^- anion, OPh should be more prone to migrate than OEt. (a) Ozerov, O. V.; Watson, L. A.; Pink, M.; Caulton, K. G. *J. Am. Chem. Soc.* **2004**, *126*, 6363. (b) The order of leaving ability of OR groups is inverse to the order of pK_a values of their conjugate acids HO R: HO^{t}Bu > HOEt > $HOSiR_3$ > HOPh (9.8).

(59) (a) The fact that $^-$O Et is a better leaving group than $^-$O^{t}Bu also contributes. (b) The β-OR elimination of (^{t}Bu$_3$SiO)$_3$TaH(CH_2CH_2OR) is much slower for R = ^{t}Bu than R = Et. See ref 18.

those of **4a**−**f**[$B(C_6F_5)_4$]/**5a**−**f**[$B(C_6F_5)_4$]. As is evident from Scheme 4, this effect could be due to changes in $k_{\beta\text{-OR}}$ or $K_{5/4}$. However, the $K_{5/4}$ values that can be measured ($K_{5a/4a}$ and $K_{5b/4b}$) are very similar for the two anions, suggesting that the difference in $k_{\beta\text{-OR,obs}}$ values is due to the $k_{\beta\text{-OR}}$ term. This is likely to be true for the other vinyl ethers **2c**−**g**, as well. One possible explanation for the anion effect is that SbF_6^-, which is more strongly coordinating than $B(C_6F_5)_4^-$, may bind weakly to **4**, increasing the effective steric crowding and accelerating β-OR elimination.[60] This is consistent with the observation that sterically bulky α-diimine ligands promote β-OR elimination rate of the SbF_6^- salts compared to $B(C_6F_5)_4^-$ salts of (α-diimine)$PdCH_2CHMeOR^+$ and explains the anion effect on the product distribution in the multiple insertion reactions in Scheme 2.[21]

Conclusions

The Brookhart olefin polymerization catalyst (α-diimine)PdMe$^+$ (**1**) reacts with vinyl ethers by two general pathways. First, **1** initiates the cationic polymerization of vinyl ethers **2a**−**c**. This pathway results in the decomposition of **1** to Pd^0. Second, **1** reacts with stoichiometric quantities of **2a**−**g** by π complex formation, insertion, chain-walking, β-OR elimination, and allylic C−H activation to form (α-diimine)Pd(η^3-C_3H_5)$^+$ (**6**) and ROH. For silyl vinyl ethers **2d**−**f**, the β-OR elimination is sufficiently slow that up to three sequential vinyl ether insertions can occur prior to β-OR elimination.

The cationic vinyl ether polymerization and associated Pd^0 formation and the β-OR elimination to form Pd allyl species that are unreactive for olefin insertion are catalyst deactivation processes that must be avoided in order to achieve **1**-catalyzed olefin/vinyl ether copolymerization. The copolymerization of 1-hexene with CH_2═CHOSiPh_3 (**2f**) by **1** is possible because insertion is much faster than cationic polymerization and β-OR elimination is relatively slow for this vinyl ether. However, the more electron-rich vinyl ethers **2a**−**c** are not suitable comonomers for **1** because for these substrates cationic polymerization out-competes insertion, and aryl vinyl ethers are unsuitable because β-OAr elimination is fast. The ability to strongly influence the reactivity of vinyl ethers with metal catalysts by modification of the vinyl ether structure, combined with the ability to tune catalyst behavior by modification of the ancillary ligands and anions, may enable broad use of vinyl ethers as comonomers in insertion polymerization of olefins.

Experimental Section

Methods and Materials. All manipulations were performed using drybox or Schlenk techniques under purified nitrogen or on a high-vacuum line unless indicated otherwise. Nitrogen was purified by passage through activated molecular sieves and Q-5 oxygen scavenger. Dichloromethane was dried over CaH_2, stored over P_2O_5, and freshly vacuum transferred prior to use. Tetrahydrofuran was distilled from sodium/benzophenone. Pentane, hexanes, toluene, and benzene were either distilled from sodium/benzophenone or purified by passage through activated alumina and BASF R3-11 oxygen removal catalyst. CD_2Cl_2 and $CDCl_3$ were degassed by three freeze−pump−thaw cycles and dried over P_2O_5. 2,6-Di-*tert*-butylpyridine was degassed by three freeze−pump−thaw cycles and distilled from CaH_2 under reduced pressure. (cod)$PdCl_2$ (cod = 1, 5-cyclooctadiene),[61] (cod)PdMeCl,[62] (α-diimine)PdMeCl (α-diimine = (2,6-(^{i}Pr)$_2$$C_6H_3$)N═CMeCMe═N(2,6-(^{i}Pr)$_2$$C_6H_3$)),[22] (α-diimine)PdMe($OEt_2$)][$SbF_6$],[22,63] [($\eta^3$-$C_3H_5$)Pd($\mu$-Cl)]$_2$,[64] and (tmeda)Pd$(OPh)_2$[43] were prepared by literature procedures. KOPh was synthesized by the reaction of KN$(SiMe_3)_2$ and phenol in THF and purified by washing with hexanes. [Li(Et_2O)$_n$][$B(C_6F_5)_4$] and [$HNMe_2Ph$][$B(C_6F_5)_4$] were obtained from Boulder Scientific. The Et_2O content in [Li(Et_2O)$_n$][$B(C_6F_5)_4$] was determined by ^{1}H NMR with C_6Me_6 as internal standard (n = 2.8). CH_2═CHO^tBu, CH_2═CHOEt, and CH_2═CHOSiMe_3 were obtained from Aldrich, degassed by three freeze−pump−thaw cycles, and dried over CaH_2. CH_2═CHOSiMe_2Ph,[65] CH_2═CHOSi$MePh_2$,[65] CH_2═CHOSiPh_3,[65] and CH_2═CHOPh[66] were prepared using literature procedures. All other chemicals were purchased from Aldrich and used without further purification.

NMR spectra were recorded on Bruker DMX-500 or DRX-400 spectrometers in Teflon-valved tubes at 20 °C unless specified otherwise. ^{1}H and ^{13}C chemical shifts are reported relative to $SiMe_4$ and were determined by reference to the residual solvent signals. Coupling constants are reported in hertz. For H_2C═CHX substrates, H_{cis} is the H that is cis to H_{int} and H_{trans} is the H that is trans to H_{int}. ^{13}C NMR resonances were assigned with the assistance of DEPT-135 experiments. The NMR spectra of $B(C_6F_5)_4^-$ salts contain signals for the free $B(C_6F_5)_4^-$ anion. ^{13}C{^{1}H} NMR (CD_2Cl_2): δ 148.5 (d, J = 242), 137.0 (d, J = 247), 135.6 (d, J = 244), 123.1 (br, C_{ipso}). ^{13}C{^{1}H} NMR (CD_2Cl_2, −60 °C): δ 147.4 (d, J = 238), 137.7 (d, J = 244), 135.8 (d, J = 236), 123.2 (br, C_{ipso}). ^{19}F NMR (CD_2Cl_2): δ −132.1 (br s, 8F, F_{ortho}), −161.3 (t, J = 20, 4F, F_{para}), −165.2 (t, J = 18, 8F, F_{meta}). ^{19}F NMR (CD_2Cl_2, −70 °C): δ −132.5 (br s, 8F, F_{ortho}), −161.7 (t, J = 20, 4F, F_{para}), −164.9 (t, J = 18, 8F, F_{meta}). ^{11}B NMR (CD_2Cl_2): δ −16.1 (br s). ^{11}B NMR (CD_2Cl_2, −70 °C): δ −15.8 (br s).

Electrospray mass spectra (ESI-MS) were recorded on freshly prepared samples (ca. 1 mg/mL in CH_2Cl_2) using an Agilent 1100 LC-MSD spectrometer incorporating a quadrupole mass filter with an m/z range of 0−3000. Typical instrumental parameters included the following: drying gas temperature 350 °C, nebulizer pressure 35 psi, drying gas flow 12.0 L/min, and fragmentor voltage 0, 70, or 100 V. In all cases where assignments are given, the observed isotope patterns closely matched calculated isotope patterns. The listed m/z value corresponds to the most intense peak in the isotope pattern.

Polymerization of CH_2═CHO^tBu (2a) by 1[$B(C_6F_5)_4$]. An NMR tube was charged with (α-diimine)PdMeCl (13.6 mg, 0.0242 mmol), [Li(Et_2O)$_{2.8}$][$B(C_6F_5)_4$] (22.0 mg, 0.0246 mmol), and 2,6-di-*tert*-butylpyridine (9.2 mg, 0.048 mmol). CD_2Cl_2 (0.4 mL) and **2a** (0.68 mmol) were added by vacuum transfer at −196 °C. The tube was warmed to 20 °C, shaken vigorously, and monitored periodically by NMR. ^{1}H NMR spectra showed that −[CH_2CH(O^tBu)]$_n$− had formed within 5 min, and **2a** was quantitatively converted to polymer after 20 h. Key NMR data for −[CH_2CH(O^tBu)]$_n$−. ^{1}H NMR ($CDCl_3$): δ 9.70 (m, −CH_2CH(O^tBu)CH_2C(═O)*H*), 5.53 (br, −CH_2CH(O^tBu)CH═C*H*CH_2−), 5.40 (br, −CH_2CH(O^tBu)C*H*═$CHCH_2$−), 4.90 (br m, −CH_2C*H*(O^tBu)$_2$), 4.00 (br, −CH_2C*H*(O^tBu)CH═$CHCH_2$−), 3.65 (CH_3C*H*(O^tBu)−), 3.59 (br, −[CH_2C*H*(O^tBu)]$_n$−), 2.35 (−CH_2CH(O^tBu)CH═CHC*H*H′−), 1.63 (br, −[C*H*$_2$CH(O^tBu)]$_n$−), 1.60 (−C*H*$_2$CH(O^tBu)CH═$CHCH_2$−), 1.45 (−C*H*$_2$CH(O^tBu)$_2$),

(60) (a) Macchioni, A.; Bellachioma, G.; Cardaci, G.; Travaglia, M.; Zuccaccia, C.; Milani, B.; Corso, G.; Zangrando, E.; Mestroni, G.; Carfagna, C.; Formica, M. *Organometallics* **1999**, *18*, 3061. (b) Zuccaccia, C.; Macchioni, A.; Orabona, I.; Ruffo, F. *Organometallics* **1999**, *18*, 4367. (c) Macchioni, A.; Magistrato, A.; Orabona, I.; Ruffo, F.; Rothlisberger, U.; Zuccaccia, C. *New J. Chem.* **2003**, *27*, 455. (d) Macchioni, A. *Eur. J. Inorg. Chem.* **2003**, 195.

(61) Drew, D.; Doyle, J. R. *Inorg. Synth.* **1990**, *28*, 348.
(62) Rülke, R. E. *Inorg. Chem.* **1993**, *32*, 5769.
(63) McCord, E. F.; McLain, S. J.; Nelson, L. T. J.; Arthur, S. D.; Coughlin, E. B.; Ittel, S. D.; Johnson, L. K.; Tempel, D.; Killian, C. M.; Brookhart, M. *Macromolecules* **2001**, *34*, 362.
(64) Tatsuno, Y.; Yoshida, T.; Otsuka, S. *Inorg. Synth.* **1990**, *28*, 342.
(65) Schaumann, E.; Tries, F. *Synthesis* **2002**, *2*, 191.
(66) Okimoto, Y.; Sakaguchi, S.; Ishii, Y. *J. Am. Chem. Soc.* **2002**, *124*, 1590.

1.36 ($CH_3CH_2CH(O^tBu)-$), 1.19 (br, $-[CH_2CH(O^tBu)]_n-$), 1.10 ($CH_3CH(O^tBu)-$), 0.78 ($CH_3CH_2CH(O^tBu)-$). $^1H-^1H$ COSY correlations ($CDCl_3$): δ/δ 5.53 (br, $-CH_2CH(O^tBu)CH{=}CHCH_2-$)/2.35 ($-CH_2CH(O^tBu)CH{=}CHCHH'-$), 5.40 (br, $-CH_2CH(O^tBu)CH{=}CHCH_2-$)/4.00 (br, $-CH_2CH(O^tBu)CH{=}CHCH_2-$), 4.90 (br m, $-CH_2CH(O^tBu)_2$)/1.45 ($-CH_2CH(O^tBu)_2$), 3.65 ($CH_3CH(O^tBu)-$)/1.10 ($CH_3CH(O^tBu)-$), 3.59 (br, $-[CH_2CH(O^tBu)]_n-$)/1.63 (br, $-[CH_2CH(O^tBu)]_n-$), 1.36 ($CH_3CH_2CH(O^tBu)-$)/0.78 ($CH_3CH_2CH(O^tBu)-$). $^{13}C\{^1H\}$ NMR ($CDCl_3$): δ 73.2 (br, $-CH_2CH(OCMe_3)-$), 67.6 (br, *mm* $-CH_2CH(O^tBu)-$), 67.2 (br, *mr* $-CH_2CH(O^tBu)-$), 66.5 (br, *rr* $-CH_2CH(O^tBu)-$), 45.6 (br, $-CH_2CH(O^tBu)-$), 29.6 (br, $-CH_2CH(OCMe_3)-$); mm/mr/rr = 1:3:1.

Generation of [(α-Diimine)PdMe(CH$_2$=CHO^{t}Bu)][SbF$_6$] (3a[SbF$_6$]). An NMR tube was charged with **1**[SbF_6] (20.0 mg, 0.0237 mmol), and CD_2Cl_2 (0.4 mL) and **2a** (0.024 mmol) were added by vacuum transfer at −196 °C. The tube was warmed to −78 °C, shaken to dissolve and thoroughly mix the components, and placed in an NMR probe that had been precooled to −60 °C. NMR spectra at −60 °C showed that **3a**[SbF_6] (90%) had formed. ^1H NMR (CD_2Cl_2, −60 °C): δ 7.37−7.28 (m, 6H), 7.09 (dd, J = 13, 4, 1H, H_{int}), 3.27 (d, J = 13, 1H, H_{trans}), 2.96 (d, J = 4, 1H, H_{cis}), 2.92 (m, 1H, C*H*Me$_2$), 2.87 (m, 2H, C*H*Me$_2$), 2.72 (m, 1H, C*H*Me$_2$), 2.30 (s, 3H, N=C*Me*), 2.23 (s, 3H, N=C*Me*), 1.41 (d, J = 7, 3H, CH*Me$_2$*), 1.35 (s, 9H, OC*Me$_3$*), 1.32 (d, J = 7, 3H, CH*Me$_2$*), 1.26 (d, J = 7, 3H, CH*Me$_2$*), 1.24 (d, J = 7, 3H, CH*Me$_2$*), 1.16 (d, J = 7, 3H, CH*Me$_2$*), 1.15 (d, J = 7, 3H, CH*Me$_2$*), 1.14 (d, J = 7, 3H, CH*Me$_2$*), 1.08 (d, J = 7, 3H, CH*Me$_2$*), 0.14 (s, 3H, Pd*Me*). $^{13}C\{^1H\}$ NMR (CD_2Cl_2, −60 °C): δ 179.3 (N=*C*Me), 175.3 (N=*C*Me), 148.2 ($CH_2{=}CHO^tBu$), 139.4, 139.0, 138.2, 137.8, 137.6, 137.1, 128.09, 128.06, 124.65, 124.62, 124.13, 124.11, 83.6 (OCMe$_3$), 54.4 ($CH_2{=}CHO^tBu$), 28.8, 28.6, 28.41, 28.36, 27.5, 24.4, 24.0 (2C), 23.9, 23.5, 23.4, 22.9, 22.8, 21.6, 16.7 (Pd*Me*).

Generation of [(α-Diimine)PdMe(CH$_2$=CHO^{t}Bu)][B(C$_6$F$_5$)$_4$] (3a[B(C$_6$F$_5$)$_4$]). An NMR tube was charged with (α-diimine)PdMeCl (12.0 mg, 0.0214 mmol) and [Li(Et$_2$O)$_{2.8}$][B(C$_6$F$_5$)$_4$] (20.2 mg, 0.0226 mmol). CD_2Cl_2 (0.4 mL) was added by vacuum transfer at −196 °C. The tube was warmed to 20 °C and shaken for 10 min. **2a** (0.04 mmol) was added by vacuum transfer at −196 °C. The tube was kept at 0 °C for 10 min. The volatiles were evacuated, and CD_2Cl_2 (0.4 mL) was added by vacuum transfer at −196 °C. The tube was warmed to 20 °C, shaken vigorously, and monitored periodically by NMR. NMR analysis showed a mixture of [{(α-diimine)PdMe}$_2$(μ-Cl)]$^+$ (8%), **3a**[B(C$_6$F$_5$)$_4$] (78%), [(α-diimine)Pd{CH$_2$CHMe(O^{t}Bu)}][B(C$_6$F$_5$)$_4$] (**4a**[B(C$_6$F$_5$)$_4$], 10%), and [(α-diimine)Pd{CMe$_2$(O^{t}Bu)}][B(C$_6$F$_5$)$_4$] (**5a**[B(C$_6$F$_5$)$_4$], 4%) after 10 min. The NMR spectra of **3a**[B(C$_6$F$_5$)$_4$] are very similar to those of **3a**[SbF_6].

Generation of 4a[B(C$_6$F$_5$)$_4$] and 5a[B(C$_6$F$_5$)$_4$]. An NMR tube was charged with (α-diimine)PdMeCl (12.0 mg, 0.0214 mmol) and [Li(Et$_2$O)$_{2.8}$][B(C$_6$F$_5$)$_4$] (20.2 mg, 0.0226 mmol). CD_2Cl_2 (0.4 mL) was added by vacuum transfer at −196 °C. The tube was warmed to 20 °C and shaken for 10 min. **2a** (0.04 mmol) was added by vacuum transfer at −196 °C. The tube was kept at 0 °C for 10 min. The volatiles were evacuated, and CD_2Cl_2 (0.4 mL) was added by vacuum transfer at −196 °C. The tube was warmed to 20 °C, shaken vigorously, and monitored periodically by NMR. NMR analysis showed that, after 2 h, a mixture of **3a**[B(C$_6$F$_5$)$_4$] (3%), **4a**[B(C$_6$F$_5$)$_4$] (66%), and **5a**[B(C$_6$F$_5$)$_4$] (25%) was present. After 22 h, the consumption of **3a**[B(C$_6$F$_5$)$_4$] was complete, and **4a**[B(C$_6$F$_5$)$_4$] (59%), **5a**[B(C$_6$F$_5$)$_4$] (22%), and [(α-diimine)Pd(η^3-C_3H_5)][B(C$_6$F$_5$)$_4$] (**6**[B(C$_6$F$_5$)$_4$], 16%) were present. ESI-MS of (α-diimine)Pd{CH$_2$CH(O^{t}Bu)Me}$^+$ and (α-diimine)Pd{CMe$_2$(O^{t}Bu)}$^+$: calcd m/z = 625.3, found 625.2. The aromatic ^1H NMR resonances of **4a**[B(C$_6$F$_5$)$_4$] and **5a**[B(C$_6$F$_5$)$_4$] overlap, and the ^{13}C NMR resonances of these species are very similar and therefore only key NMR data are listed.[67] Key NMR data for **4a**[B(C$_6$F$_5$)$_4$]. ^1H NMR (CD_2Cl_2): δ 4.86 (m, 1H, PdCH$_2$C*H*Me(O^{t}Bu)), 3.79 (sept, J = 7, 1H, C*H*Me$_2$), 3.29 (sept, J = 7, 1H, C*H*Me$_2$), 2.93 (sept, J = 7, 1H, C*H*Me$_2$), 2.61 (sept, J = 7, 1H, C*H*Me$_2$), 2.20 (s, 3H, N=C*Me*), 2.17 (s, 3H, N=C*Me*), 0.93 (t, J = 7, 1H, PdC*H*H′CHMe(O^{t}Bu)), 0.85 (s, 9H, OC*Me$_3$*), 0.40 (dd, J = 7, 4, 1H, PdCH*H*′CHMe(O^{t}Bu)). The PdCH$_2$CH*Me*(O^{t}Bu) signal is obscured but was identified by COSY NMR at δ 1.22. $^1H-^1H$ COSY correlations (CD_2Cl_2, −40 °C): δ/δ 4.83 (PdCH$_2$C*H*Me(O^{t}Bu))/1.22 (PdCH$_2$CH*Me*(O^{t}Bu)), 4.83(PdCH$_2$C*H*Me(O^{t}Bu))/0.81 (PdC*H*H′CHMe(O^{t}Bu)), 4.83 (PdCH$_2$C*H*Me(O^{t}Bu))/0.27 (PdCH*H*′CHMe(O^{t}Bu)), 0.81 (PdC*H*H′-CHMe(O^{t}Bu))/0.27 (PdCH*H*′CHMe(O^{t}Bu)). ^1H NMR ($CDCl_2F$, −130 °C): δ 4.85 (m, 1H, PdCH$_2$C*H*Me(O^{t}Bu)), 3.96 (m, J = 7, 1H, C*H*Me$_2$), 3.32 (sept, J = 7, 1H, C*H*Me$_2$), 2.84 (sept, J = 7, 1H, C*H*Me$_2$), 2.46 (sept, J = 7, 1H, C*H*Me$_2$), 0.78 (s, 9H, OC*Me$_3$*). $^{13}C\{^1H\}$ NMR (CD_2Cl_2, −40 °C): δ 88.9 (OCMe$_3$), 88.3 (PdCH$_2$*C*HMe(O^{t}Bu)), 9.3 (Pd*C*H$_2$CHMe(O^{t}Bu)). Key NMR data for **5a**[B(C$_6$F$_5$)$_4$]. ^1H NMR (CD_2Cl_2): δ 3.05 (sept, J = 7, 4H, C*H*Me$_2$), 2.21 (s, 3H, N=C*Me*), 2.20 (s, 3H, N=C*Me*), 1.11 (s, 9H, OC*Me$_3$*), 0.64 (s, 6H, PdC*Me$_2$*(O^{t}Bu)). ^1H NMR ($CDCl_2F$, −130 °C): δ 3.02 (sept, J = 7, 4H, C*H*Me$_2$), 1.07 (s, 9H, OC*Me$_3$*), 0.63 (s, 6H, C*Me$_2$*). $^{13}C\{^1H\}$ NMR (CD_2Cl_2, −40 °C): δ 90.3 (OCMe$_3$), 82.8 (Pd*C*Me$_2$(O^{t}Bu)).

The first-order rate constant for the consumption of **3a**[B(C$_6$F$_5$)$_4$] ($k_{insert,\ 3a}$) was measured by the disappearance of the Pd*Me* resonance of **3a**[B(C$_6$F$_5$)$_4$] and increase of the PdCH$_2$C*H*Me resonance of **4a**[B(C$_6$F$_5$)$_4$] plus the PdC*Me$_2$* resonance of **5a**[B(C$_6$F$_5$)$_4$]. The equilibrium constant $K_{5/4}$ was determined from the ratio of the integrated intensities of the PdC*Me$_2$* resonance of **5a**[B(C$_6$F$_5$)$_4$] and the PdCH$_2$C*H*Me resonance of **4a**[B(C$_6$F$_5$)$_4$].

Reaction of 4a[B(C$_6$F$_5$)$_4$]/5a[B(C$_6$F$_5$)$_4$] with MeCN. An NMR tube containing a CD_2Cl_2 solution (0.4 mL) of **4a**[B(C$_6$F$_5$)$_4$] (0.016 mmol) and **5a**[B(C$_6$F$_5$)$_4$] (0.0055 mmol) was frozen at −196 °C, and MeCN (0.026 mmol) was added by vacuum transfer. The tube was warmed to −78 °C, agitated to mix the components, placed in an NMR probe that had been precooled to −60 °C, and monitored by NMR. ^1H NMR spectra showed that, after 5 min, **4a**[B(C$_6$F$_5$)$_4$] had been consumed, and a mixture of **5a**[B(C$_6$F$_5$)$_4$] (24%) and [**4a**-MeCN][B(C$_6$F$_5$)$_4$] (76%) was present. The tube was then warmed to −40 °C and monitored periodically by NMR. After 140 min, a mixture of **5a**[B(C$_6$F$_5$)$_4$] (5%) and [**4a**-MeCN][B(C$_6$F$_5$)$_4$] (91%) was present. Exchange between free and coordinated MeCN is slow on the NMR time scale at −40 °C. Compound **4a**[B(C$_6$F$_5$)$_4$] was not detected during this reaction. Data for [**4a**-MeCN][B(C$_6$F$_5$)$_4$]. ^1H NMR (CD_2Cl_2, −40 °C): δ 7.42−7.26 (m, 6H), 3.18 (m, 1H, PdCH$_2$C*H*Me(O^{t}Bu)), 2.90 (m, 2H, C*H*Me$_2$), 2.83 (m, 2H, C*H*Me$_2$), 2.21 (s, 3H, N=C*Me*), 2.19 (s, 3H, N=C*Me*), 1.71 (s, 3H, *Me*CN), 1.53 (m, 1H, PdC*H*H′CHMe(O^{t}Bu)), 1.31 (d, J = 6, 12H, CH*Me$_2$*), 1.15 (d, J = 6, 6H, CH*Me$_2$*), 1.10 (3H, CH*Me$_2$*), 1.08 (3H, CH*Me$_2$*), 0.97 (d, J = 6, 3H, PdCH$_2$CH*Me*(O^{t}Bu)), 0.84 (s, 9H, OC*Me$_3$*). The other PdCH*H*′ signal is obscured but was identified by COSY NMR at δ 1.15. Key $^1H-^1H$ COSY correlations (CD_2Cl_2, −40 °C, NMR 500−2, 45−126) δ/δ: 3.18 (PdCH$_2$C*H*Me(O^{t}Bu))/1.53 (PdC*H*H′CHMe(O^{t}Bu)), 3.18 (PdCH$_2$C*H*Me(O^{t}Bu))/1.15 (PdCH*H*′CHMe(O^{t}Bu)), 3.18 (PdCH$_2$C*H*Me(O^{t}Bu))/0.97 (PdCH$_2$CH*Me*(O^{t}Bu)), 1.53 (PdC*H*H′CHMe(O^{t}Bu))/1.15 (PdCH*H*′CHMe(O^{t}Bu)). $^{13}C\{^1H\}$ NMR (CD_2Cl_2, −40 °C): δ 179.8 (N=*C*Me), 172.1 (N=*C*Me), 139.7, 139.4, 138.4, 138.2, 137.4 (2C), 128.9, 128.1, 124.7, 124.6, 124.1, 124.0, 121.8, 72.8 (OCMe$_3$), 67.2 (PdCH$_2$*C*HMe(O^{t}Bu)), 36.9 (Pd*C*H$_2$CHMe(O^{t}Bu)), 28.95, 28.92, 28.7, 28.6, 27.8, 25.6, 23.8, 23.6, 23.3, 23.2, 23.1, 23.0 (2C), 22.8, 22.2, 20.0, 2.0 (*Me*CN).

(67) $^{13}C\{^1H\}$ NMR of [(α-diimine)Pd{CH$_2$CHMe(O^{t}Bu)}][B(C$_6$F$_5$)$_4$] and [(α-diimine)Pd{CMe$_2$(O^{t}Bu)}][B(C$_6$F$_5$)$_4$]: δ 178.1, 174.5, 171.6, 143.4, 142.8, 141.6, 140.9, 138.5, 137.8, 137.5, 137.0, 136.5, 136.2, 128.7, 128.1, 127.9, 127.6, 124.54, 124.48, 124.41, 124.36 (2C), 124.2, 90.3, 88.9, 88.3, 82.9, 30.6, 29.7, 29.04, 28.99, 28.95, 28.75, 28.65, 28.6, 26.2, 25.5, 24.5, 24.0, 23.8, 23.7, 23.29, 23.25, 22.9, 22.8, 22.6, 22.5, 22.3, 21.2, 21.1, 20.0, 19.5, 9.3. One of the N=*C*Me resonances of [(α-diimine)Pd{CMe$_2$(O^{t}Bu)}][B(C$_6$F$_5$)$_4$] was obscured, and the OC*Me$_3$* resonances for [(α-diimine)Pd{CH$_2$CHMe(O^t*Bu*)}][B(C$_6$F$_5$)$_4$] and [(α-diimine)Pd{CMe$_2$(O^t*Bu*)}][B(C$_6$F$_5$)$_4$] overlap.

Conversion of 4a[B(C$_6$F$_5$)$_4$]/5a[B(C$_6$F$_5$)$_4$] to 6[B(C$_6$F$_5$)$_4$]. An NMR tube containing a CD_2Cl_2 solution of **4a**[B(C$_6$F$_5$)$_4$] (0.038 mmol) and **5a**[B(C$_6$F$_5$)$_4$] (0.014 mmol) was maintained at 20 °C and monitored by NMR periodically. Over the course of 15 days, 90% of **4a**[B(C$_6$F$_5$)$_4$] and **5a**[B(C$_6$F$_5$)$_4$] were converted to **6**[B(C$_6$F$_5$)$_4$] and HO^{t}Bu. The first-order rate constant for consumption of the total of **4a**[B(C$_6$F$_5$)$_4$] and **5a**[B(C$_6$F$_5$)$_4$] was measured by the disappearance of the sum of the PdCH$_2$C*H*Me resonance of **4a**[B(C$_6$F$_5$)$_4$] and the PdC*Me*$_2$ resonance of **5a**[B(C$_6$F$_5$)$_4$]. **6**[B(C$_6$F$_5$)$_4$] was prepared by the procedure reported by Risse for the analogous compound [(2,2′-bipyridyl)Pd(η^3-C$_3$H$_5$)][SbF$_6$] and characterized by X-ray diffraction (see Supporting Information).[68] NMR data for **6**[B(C$_6$F$_5$)$_4$]. ^{1}H NMR (CD_2Cl_2): δ 7.41−7.32 (m, 6H), 5.65 (m, 1H, H$_{int}$), 3.36 (d, J = 7, 2H, H$_{syn}$), 3.04 (d, J = 13, 2H, H$_{anti}$), 2.96 (sept, J = 7, 2H, C*H*Me$_2$), 2.70 (sept, J = 7, 2H, C*H*Me$_2$), 2.26 (s, 6H, N=C*Me*), 1.35 (d, J = 7, 6H, CH*Me*$_2$), 1.26 (d, J = 7, 6H, CH*Me*$_2$), 1.23 (d, J = 7, 6H, CH*Me*$_2$), 1.21 (d, J = 7, 6H, CH*Me*$_2$). ^{13}C{^{1}H} NMR (CD_2Cl_2): δ 176.9 (N=*C*Me), 144.0, 137.1, 137.0, 129.1, 125.0, 125.0, 121.1, 65.8 (allyl *C*H$_2$), 29.8, 29.5, 23.7, 23.6, 23.4, 23.3, 20.1. ESI-MS of (α-diimine)Pd(η^3-C$_3$H$_5$)$^+$: calcd m/z = 551.3, found 551.2. Anal. Calcd for C$_{55}$H$_{45}$BF$_{20}$N$_2$Pd: C, 53.66; H, 3.68; N, 2.28. Found: C, 53.78; H, 3.67; N, 2.19.

The first-order rate constant for consumption of the total of **4a**[B(C$_6$F$_5$)$_4$] and **5a**[B(C$_6$F$_5$)$_4$], $k_{\beta\text{-O}^t\text{Bu,obs}}$, was measured by the disappearance of the PdCH$_2$C*H*Me ^{1}H NMR resonance of **4a**[B(C$_6$F$_5$)$_4$] plus the PdC*Me*$_2$ ^{1}H NMR resonance of **5a**[B(C$_6$F$_5$)$_4$] and the increase in the H_{int} resonance of **6**[B(C$_6$F$_5$)$_4$].

Insertion of 3a[SbF$_6$] and Reactions of 1 with 2b−g. The insertion rate constant of **3a**[SbF$_6$], the equilibrium constant between **5a**[SbF$_6$] and **4a**[SbF$_6$], and the β-O^{t}Bu elimination rate constant of **5a**[SbF$_6$]/**4a**[SbF$_6$] were measured by the methods described above for the B(C$_6$F$_5$)$_4^-$ salts. The reactions of **1**[SbF$_6$] and **1**[B(C$_6$F$_5$)$_4$] with **2b−g** were studied using the procedures described above for **2a**. Full details are provided in the Supporting Information.

Competitive Binding of Ethylene and CH$_2$=CHOR (2a−c) to 1[SbF$_6$] (eq 4). The procedure for **2a** is described here; an identical procedure was used for **2b**,**c**. An NMR tube was charged with **1**[SbF$_6$] (15.0 mg, 0.0179 mmol). CD_2Cl_2 (0.4 mL) was added by vacuum transfer at −196 °C. The tube was warmed to 20 °C and shaken. Ethylene (0.062 mmol) and **2a** (0.040 mmol) were added by vacuum transfer at −196 °C. The tube was warmed to −78 °C, shaken, and placed in an NMR probe that had been precooled to −60 °C. The reaction was monitored periodically by ^{1}H NMR at −60 °C until the reaction quotient $Q_{\mathbf{2a}/\text{ethylene}}$ = [**3a**][CH$_2$=CH$_2$][(α-diimine)PdMe(CH$_2$=CH$_2$)$^+$]$^{-1}$[**2a**]$^{-1}$ reached a constant value. Additional **2a** (0.062 mmol) was added by vacuum transfer to change the ethylene/**2a** ratio, and the tube was monitored by ^{1}H NMR at −60 °C until $Q_{\mathbf{2a}/\text{ethylene}}$ again reached a constant value. This process was repeated one more time, and the average $K_{\mathbf{2a}/\text{ethylene}}$ (SbF$_6^-$) value is reported in Table 2. The competitive binding of **2d−g** and **2c** to **1**[SbF$_6$] at −20 °C (eq 5) and of ethylene and CH$_2$=CHOR (**2a-c**, **2g**) to **1**[B(C$_6$F$_5$)$_4$] at −60 °C (eq 4) was studied in a similar manner.

Generation of [{(tmeda)Pd(OPh)}$_n$][B(C$_6$F$_5$)$_4$]$_n$ (7). An NMR tube was charged with (tmeda)Pd(OPh)$_2$ (10.9 mg, 0.0267 mmol), [HNMe$_2$Ph][B(C$_6$F$_5$)$_4$] (21.6 mg, 0.0270 mmol), and CD_2Cl_2 (0.4 mL) was added by vacuum transfer at −196 °C. The tube was warmed to 20 °C and shaken vigorously. NMR spectra showed that [{(tmeda)Pd(OPh)}$_n$][B(C$_6$F$_5$)$_4$]$_n$, NMe$_2$Ph, and HOPh had formed quantitatively in 10 min.[69] The ESI-MS contains signals for only the mononuclear monocation (tmeda)Pd(OPh)$^+$ even at low fragmentor volatage, while ^{1}H PGSE NMR experiments suggest a tetrameric structure (n = 4), referencing [(tmeda)Pd(OPh)(NCMe)][B(C$_6$F$_5$)$_4$] as a monomeric analogue.[70] These results indicate that **7** is most likely a labile oligomer in CD_2Cl_2 solution. Key NMR data for **7**. ^{1}H NMR (CD_2Cl_2): δ 7.73 (d, J = 8, 2H, H$_{ortho}$), 7.45 (t, J = 8, 2H, H$_{meta}$), 7.27 (t, J = 8, 1H, H$_{para}$), 2.46 (m, 4H, −C*H*$_2$−), 2.08 (s, 12H, N*Me*$_2$). ^{13}C{^{1}H} NMR (CD_2Cl_2): δ 158.8, 131.8, 126.1, 124.3, 64.0, 50.6. ESI-MS of (tmeda)Pd(OPh)$^+$: calcd m/z = 315.1, found 315.0.

Reaction of 7 with Propylene. The above solution of in situ generated **7** was frozen at −196 °C, and propylene (1 equiv) was added by vacuum transfer. The tube was warmed to −30 °C. ^{1}H NMR showed no reaction occurred after 30 min at −30 °C. The sample was then warmed to 20 °C. After 10 h, ^{1}H NMR showed that **7** was completely converted to [(tmeda)Pd(η^3-C$_3$H$_5$)][B(C$_6$F$_5$)$_4$] and HOPh.

[(tmeda)Pd(OPh)(NCMe)][B(C$_6$F$_5$)$_4$] ([7-MeCN][B(C$_6$F$_5$)$_4$]). A solution of in situ generated **7** in CD_2Cl_2 was frozen at −196 °C, and MeCN (1.1 equiv) was added by vacuum transfer. The tube was warmed to 20 °C and shaken. ^{1}H NMR showed that [**7**-MeCN][B(C$_6$F$_5$)$_4$] had formed quantitatively in 5 min. ^{1}H NMR (CD_2Cl_2): δ 7.11−7.06 (m, 4H), 6.69 (m, 1H, H$_{para}$), 2.78 (m, 2H, −C*H*$_2$−), 2.72 (s, 6H, N*Me*$_2$), 2.68 (s, 6H, N*Me*$_2$), 2.55 (m, 2H, −C*H*$_2$−), 2.08 (*Me*CN). ^{13}C{^{1}H} NMR (CD_2Cl_2) δ 165.9, 156.4, 129.6, 119.8, 117.2, 63.3, 62.3, 51.7, 50.9, 3.1 (*Me*CN). ESI-MS of (tmeda)Pd(OPh)(NCMe)$^+$: calcd m/z = 356.1, found 356.0.[71]

[(tmeda)Pd(η^3-C$_3$H$_5$)][B(C$_6$F$_5$)$_4$]. This species was prepared following the procedure reported by Risse for the analogous compound [(2,2′-bipyridyl)Pd(η^3-C$_3$H$_5$)][SbF$_6$].[72] ^{1}H NMR (CD_2Cl_2): δ 5.66 (m, 1H, H$_{int}$), 3.79 (d, J = 7, 2H, H$_{syn}$), 3.00 (d, J = 13, 2H, H$_{anti}$), 2.91 (s, 6H, N*Me*$_2$), 2.73 (s, 6H, N*Me*$_2$), 2.80 (m, 2H, −C*H*$_2$−), 2.71 (m, 2H, −C*H*$_2$−). ^{13}C{^{1}H} NMR (CD_2Cl_2): δ 119.8 (allyl *C*H), 61.9, 61.1, 52.5 (N*Me*$_2$), 51.9 (N*Me*$_2$). ESI-MS of (tmeda)Pd(η^3-C$_3$H$_5$)$^+$: calcd m/z = 263.1, found 263.0. Anal. Calcd for C$_{33}$H$_{21}$BF$_{20}$N$_2$Pd: C, 42.04; H, 2.25; N, 2.97. Found: C, 42.13; H, 2.31; N, 2.89.

Computational Methods. DFT computations were performed using Gaussian 03.[73] The geometries of the stationary points were found using the B3LYP functional.[74] C, H, N, and O atoms were modeled using the 6-31G* basis set,[75] and Pd and Si were modeled using the LANL2DZ basis set including the relativistic pseudopotentials of Hay and Wadt.[76]

Acknowledgment. This work was supported by the U.S. Department of Energy (DE-FG-02-00ER15036).

Supporting Information Available: Experimental procedures, characterization of complexes, details of kinetic studies, and complete ref 73. This material is available free of charge via the Internet at http://pubs.acs.org.

JA100491Y

(68) (a) Rush, S.; Reinmuth, A.; Risse, W. *Macromolecules* **1997**, *30*, 7375. (b) For [(α-diimine)Pd(η^3-C$_3$H$_5$)][3,5-(CF$_3$)$_2$C$_6$H$_3$)] see: Li, W.; Zhang, X.; Meetsma, A.; Hessen, B. *J. Am. Chem. Soc.* **2004**, *126*, 12246.

(69) NMR spectra showed that NMe$_2$Ph and HOPh are both free and do not coordinate to the [{(tmeda)Pd(OPh)}$_n$][B(C$_6$F$_5$)$_4$]$_n$ in CD_2Cl_2 at 20 °C.

(70) For the related tetrameric compound [(cod)$_4$Pt$_4$(μ^2-OH)$_4$](OTf)$_4$, see: Szuromi, E. Ph.D. Thesis, University of Missouri−Columbia, December 2005.

(71) The major peak is (tmeda)Pd(OPh)$^+$ calcd. m/z = 315.1, found 315.0.

(72) For the related compound [(tmeda)Pd(η^3-C$_3$H$_5$)]Br, see: Graff, W.; Boersma, J.; Koten, G. *Organometallics* **1990**, *9*, 1479.

(73) Frisch, M. J.; et al. *Gaussian 03*, revision C.02; Gaussian, Inc.: Wallingford, CT, 2004. See the Supporting Information for the complete citation.

(74) (a) Becke, A. D. *J. Chem. Phys.* **1993**, *98*, 5648. (b) Lee, C.; Yang, W.; Parr, R. G. *Phys. Rev. B* **1988**, *37*, 785. (c) Miehlich, B.; Savin, A.; Stoll, H.; Preuss, H. *Chem. Phys. Lett.* **1989**, *157*, 200.

(75) (a) Rassolov, V. A.; Ratner, M. A.; Pople, J. A.; Redfern, P. C.; Curtiss, L. A. *J. Comput. Chem.* **2001**, *22*, 976. (b) Rassolov, V. A.; Pople, J. A.; Ratner, M. A.; Windus, T. L. *J. Chem. Phys.* **1998**, *109*, 1223. (c) Ditchfield, R.; Hehre, W. J.; Pople, J. A. *J. Chem. Phys.* **1971**, *54*, 724.

(76) (a) Hay, P. J.; Wadt, W. R. *J. Chem. Phys.* **1985**, *82*, 270. (b) Wadt, W. R.; Hay, P. J. *J. Chem. Phys.* **1985**, *82*, 284. (c) Hay, P. J.; Wadt, W. R. *J. Chem. Phys.* **1985**, *82*, 299.